HEWLETT·PACKARD JOURNAL

Contents:

APRIL 1983 Volume 34 ● Number 4

In this Issue:

In this imperfect world of ours, there's no such thing as a straight edge, a flat surface, or parallel lines. Those who inhabit the world of precision machining are constantly reminded of these truths as designers demand tolerances just a little tighter than the newest and best machine tools can deliver. In this environment, it's essential to know just how imperfect a machine tool is. Many machine tools are computer controlled and can be programmed to compensate for errors if accurate calibration data is available.

Because today's machine tools are very, very precise, it takes a super-precise measuring tool to calibrate them. The subject of the articles on page 3 to 22, the HP 5528A Laser Measurement System, is such a tool. The LMS consists of a laser head, precision optical components, and a microcomputer-based measurement and display unit, optionally augmented with an HP-85 Computer. The cover photo shows it doing its job. The LMS is used periodically or as needed to check a machine's accuracy, to provide data for computer error compensation, to detect wear, and to diagnose problems.

Back in August 1970, HP's first laser measurement system was described in these pages as "a two-hundred-foot yardstick with graduations every microinch." The 5528A LMS retains that laser precision and offers better optics, easier setup, and more automated operation. It measures not only length or position, but also straightness, flatness, squareness, pitch, yaw, and parallelism. And it has many uses in addition to machine tool calibration—for example, in metrology laboratories and integrated circuit lithography.

Any time a signal passes through some part of a system, say an amplifier or a filter, it's likely to come out noisier than it went in. It's just another example of our imperfect world. To describe how much noise a system component adds to a signal, engineers use a figure of merit called noise figure. There are many ways to measure noise figure, some easier than others and some more accurate. It used to be that accuracy precluded convenience. If you wanted a quick noise figure measurement it was necessarily inaccurate and nonrepeatable. The HP 8970A Noise Figure Meter described in the article on page 23 is designed to change all that by measuring noise figure conveniently, accurately, and repeatably. Besides the 8970A design story, the article also gives us some basic information on noise figure and its measurement.

One of the great benefits of microprocessor control of instruments is that diagnostic programs can be built in so that instruments can test themselves. The HP 4145A Semiconductor Parameter Analyzer (see our October 1982 issue) tests itself. However, one of its subsystems, the flexible disc drive, is a purchased part, wasn't designed as part of the 4145A, and didn't come with self-test capability. In the *Laboratory Notebook* article on page 35, one of the 4145A's designers tells how the design team solved this typical engineering problem.

-R. P. Dolan

A New Microcomputer-Controlled Laser Dimensional Measurement and Analysis System

Microcomputer control simplifies machine tool calibration. Other applications are in research and development, general-purpose metrology, and surface plate calibration.

by Robert C. Quenelle and Lawrence J. Wuerz

HEWLETT-PACKARD is well known as a source of electronic instrumentation. Not so well known is that the company also makes instruments for precise distance and angle measurements. One family of these instruments uses interferometer techniques to make high-resolution measurements. The first product in this family was a laser interferometer that could measure large distances with a resolution of 10^{-8} meter or 10^{-6} inch.[1] This first interferometer found acceptance in the machine tool industry as a means of certifying and calibrating machine tool positioning systems and distance readouts.

Improvements to the original system allowed remote measurements, that is, measurements between two passive optical components.[2] Previous measurements were all made between the laser and an optical component. Along with the remote interferometer came a new angle-sensitive interferometer that allowed measuring pitch, yaw, and flatness more conveniently than with traditional autocollimator techniques. Several years later a new interferometer sensitive to straightness, or deviation from travel in a straight line, was introduced.[3] This interferometer, along with a precision optical square, proved very useful for evaluating machine tool straightness of travel, orthogonality between axes (squareness), and parallelism. Once again, the straightness interferometer replaced less accurate and less convenient conventional techniques.
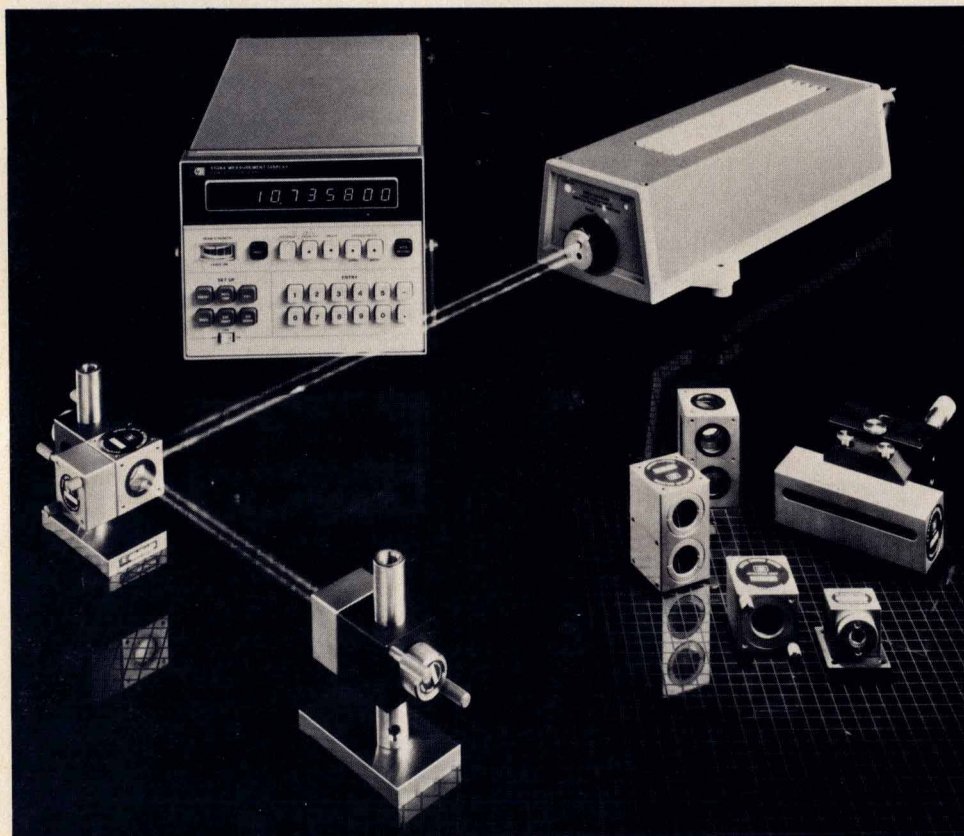
Fig. 1. *The 5528A Laser Measurement System consists of a laser head, a measurement display, and precision optical components. It measures linear position, pitch and yaw, straightness, squareness, flatness, and parallelism.*

The HP 5528A Laser Measurement System, Fig. 1, is a completely new implementation of the above measurements. It is more compact, more powerful and less expensive than the previous system. A new measurement controller and display, Model 5508A, incorporates several functions that were previously in separate boxes. Its front-panel keyboard and microprocessor provide more functions than its predecessor, and the new laser head, Model 5518A, has the straightness adapter optics built in. The new optical components are generally smaller and come with more versatile mounting hardware designed to simplify changing from one measurement to another. All of these new products were designed to be as good as the previous product line while offering higher performance when possible and a lower price.

Measurement data is available in digital form via an HP-IB (IEEE 488) port on the rear panel of the 5508A Measurement Display. This output is used by the HP 55288A Dimensional Metrology Analysis System, which includes an HP-85 Computer and special software. With the 55288A, the user receives convenient interpretation of information. Machine calibration data can be stored, plotted and analyzed. Calibration time is reduced, and complex calculations are done automatically. The 55288A System is recommended for simplifying surface plate calibrations and straightness measurements.

Accuracy of the new 5528A Laser Measurement System is typically two microinches per inch of travel and resolution is one microinch. Distances up to 120 feet may be measured.

Dimensional Metrology Software Eases Calibration

by Lawrence J. Wuerz and Christopher Burns

Calibration of machine tools using the HP 5528A Laser Measurement System can be performed much more effectively when a controller is used to assist the gathering and analyzing of data. For this reason, the 5508A is designed to allow programming and data reading via the HP-IB (IEEE 488). The HP 55288A Dimensional Metrology Analysis System is designed to simplify the calibration process by automating measurement setup and control. Based on the HP-85 Personal Computer, it is a portable package flexible enough to satisfy the differing needs of most users.

In gathering data, the computer does two things that are particularly useful. First, it records data values electronically, far more

quickly and reliably than could be done by hand. Second, it ensures that measurements are performed in an organized manner. In measuring the accuracy of a machine tool, the tool is moved to target positions at which data is taken. Usually it is required to move to and take a data point at each target several times to test the machine's repeatability. It may also be necessary to approach the targets from different directions to check the machine for hysteresis (backlash). Metrologists have developed a number of schemes for approaching the targets in various orders of data taking which optimize measurements in various ways. When the HP metrology software is used, the computer

POSITIONING ERROR PLOT

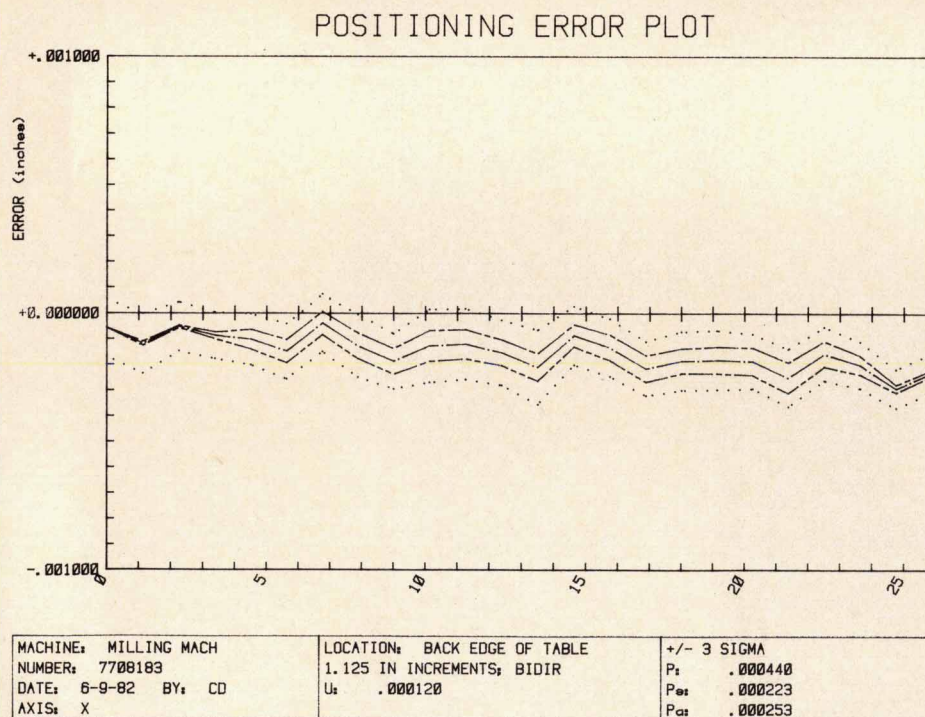| MACHINE: MILLING MACH	LOCATION: BACK EDGE OF TABLE	+/- 3 SIGMA	
NUMBER: 7708183	1.125 IN INCREMENTS; BIDIR	P:	.000440
DATE: 6-9-82 BY: CD	U: .000120	Pe:	.000223
AXIS: X		Pa:	.000253

Fig. 1. A typical linear error plot for a milling machine, produced by the 55288A Dimensional Metrology Analysis System.

keeps track of the measurements, relieving the user of this task. For example, consider how a metrology software user would measure the linear positioning accuracy of a machine tool. The software first asks for target positions. The operator can type these in individually or call for evenly spaced targets at specified intervals between specified beginning and ending points. The user then selects how many runs (i.e., readings at each target) and what order of data taking to use. Then, for each reading, the computer tells the user what target to move to and stands by to accept data. The user moves to the target using the machine's position control (i.e., the device under test) and then presses the laser system's **RECORD** key, sending the actual machine position to the computer. The computer then compares the actual position with the target position, stores the difference as error data, and prompts the user to go to the next target to be measured.

Once all the data has been collected, the metrology software offers a choice of several formats for output. If desired, the raw data can be printed out on the HP-85's internal printer for analysis. In most cases, however, metrologists want the same basic analysis: a graph of machine error versus position, showing the average of all error data taken at each target and a confidence window about that average based on the standard deviation of the data. The 5528A metrology software has the ability to generate these plots automatically on either the computer's built-in CRT or an HP-GL* plotter. An example of a linear error plot from an HP 7470A Plotter is shown in Fig. 1. The figure shows positional error versus position for a milling machine with data points taken every 1.125 inches over a 26-inch travel. The middle line (dot-dash) denotes the mean or average of all the errors at a particular position. If the data associated with this plot involved ten runs of data, this line denotes the average of all ten errors at each linear position. Since the data plotted here was gathered using an order of data taking in which targets were approached from both directions, the plot also shows the averages for the sets of data points taken in each direction separately. These are the broken lines on either side of the middle line, which show that the positioning of this machine exhibits a fair amount of hysteresis, or backlash.

*HP-GL: Hewlett-Packard Graphics Language

Plots can also be generated with both directions analyzed together, if desired. The uppermost and lowest dotted lines represent the $\pm 3\sigma$ or 99.7% confidence intervals calculated from the data at a given position. The machine should perform within these limits 99.7% of the time.

The plot in Fig. 1 conforms, in analysis and format, to the VDI 3441 specification commonly used in Europe. The metrology software can also provide similar plots conforming to the NMTBA standard used in the U.S.A.

The metrology system operates in basically the same manner for linear positioning data, angular data, or straightness data. When measuring straightness, the software can remove the slope of the axis measured, showing only out-of-straightness. It can also easily calculate the parallelism or squareness between two axes.

Capability is also provided to characterize the flatness of a surface plate or machine tool bed.[1] Flatness measurements are derived from angular data taken by the 5528A, with the angular reflector mounted on a reference baseplate with precisely spaced pads. By taking measurements along all four sides, the diagonals, and the two midlines of the surface plate with the aid of the 55288A, surface plate isometric contour plots can be generated (see Fig. 2). For a typical-size surface plate, the entire calibration can be accomplished in about one-fourth the time required by conventional methods.

Acknowledgments

We would like to acknowledge the efforts of Mike Munrow for the initial design of this software and Karen Vahtra for converting the 55288A Software for use with earlier HP laser systems.

Reference

1. J.C. Moody, "How to Calibrate Surface Plates in the Plant," The Tool Engineer, October 1955.

SURFACE PLATE CONTOUR PLOT
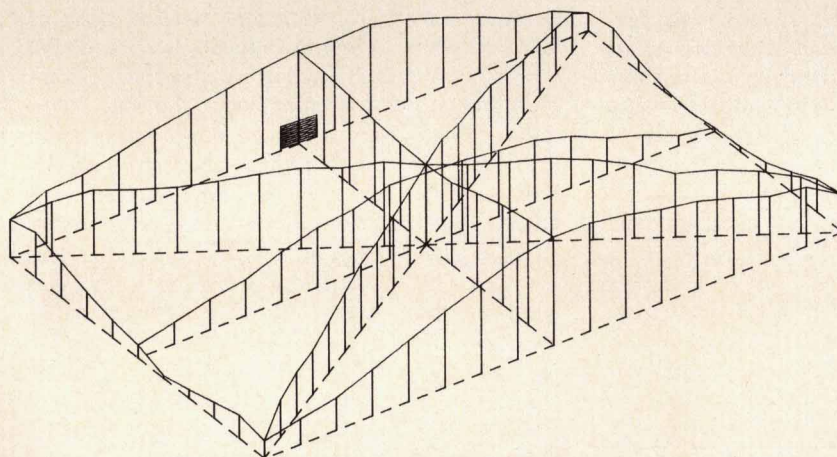
PLATE# 1021	MAX HEIGHT: +.000184 inches	CLOSURE 7 -.000014
DATE: 8-5 BY: CB	ROUTINE	CLOSURE 8 +0.000000

Fig. 2. Typical surface plate isometric contour plot.

Fig. 2. *Optical paths for a standard distance measurement. The system measures how far the movable cube corner travels during the measurement.*

Laser Measurement Theory

The 5528A Laser Measurement System uses interferometer techniques to make various measurements. Distance measurements are expl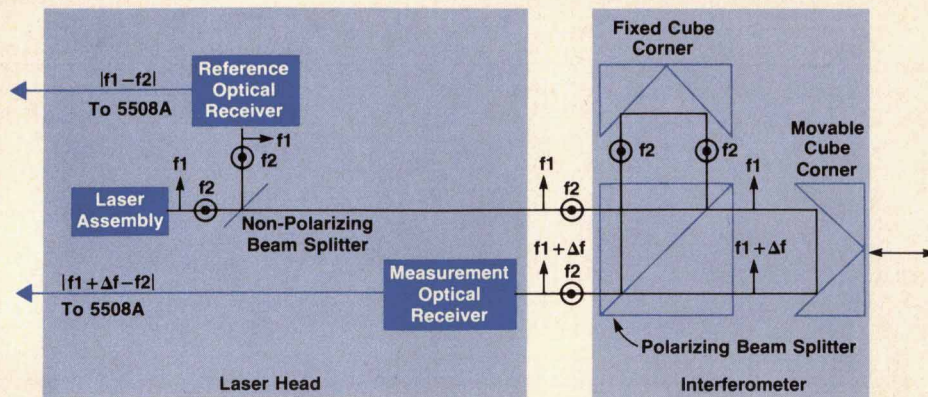ained here as an example. All HP interferometers use a two-frequency laser and polarizing optics. This combination allows stable laser tuning, provides excellent measurement range, and makes special measurements possible.

The 5518A Laser Head, described in detail later, is a source of two coaxial linearly polarized monochromatic light beams. One is polarized parallel to the 5518A mounting feet and the other is perpendicular. Their optical frequencies differ by about 2 MHz, or about 4 parts in 10^9 of the average optical frequency.

All 5528A measurements are made by converting some physical motion, such as travel along the beam axis, into changes of optical path length. Fig. 2 shows the optical path in a standard distance measurement. Inside the 5518A the two coaxial beams, shown as f1 and f2 in Fig. 2, are sampled and a portion of each is sent to the reference optical receiver. The receiver outputs a signal at the difference frequency between the two components, $|f1-f2|$. In the interferometer, a polarizing beam splitter separates the two beams. In Fig. 2, f1 is directed into the variable path of the interferometer and f2 into the fixed path. f2 strikes a reflector called a cube corner, which returns it parallel to its original direction but with an offset. f1 strikes a movable cube corner. Both beams return to the beam splitter where they recombine as a single coaxial beam. This beam returns to the 5518A and the frequency difference of the two components is measured by the measurement optical receiver.

If the measurement cube corner moves, f1 is shifted according to the Doppler effect and the beam returns at a different frequency, indicated as $f1+\Delta f$. To look at this another way, each time the cube corner moves away from the beam splitter by one-half wavelength, the optical path increases by one wavelength (one fringe in optical terminology) and one cycle of f1 does not return to the measurement receiver. This temporarily lowers the frequency of f1. The 5508A receives the outputs of both receivers and counts them in two forward counters, thus integrating the frequencies. By subtracting the contents of one counter from the other, the 5508A does the following operation:

$$\int_0^T (f1 + \Delta f - f2)dt - \int_0^T (f1 - f2)dt = \int_0^T \Delta f\, dt$$

This result represents the change in path length that has occurred since the counters were reset.

To refine the measurements further, the 5508A can automatically correct for wavelength variations caused by atmospheric conditions and can scale the measured distance to standard temperature (20°C=68°F) based on the measured material's temperature and expansion coefficient.

Measurement Display

The 5508A Measurement Display provides the operator interface for making dimensional measurements with the 5528A Laser Measurement System. It is designed to be user-friendly, to simplify the process of calibrating machines, and to act as the center of all measurement activity. It contains special counters for processing the reference and measurement (Doppler) frequencies returning from the 5518A Laser Head, analog-to-digital circuitry for processing automatic wavelength compensation information, a keyboard with numeric keypad for easy entry of measurement parameters, HP-IB circuitry, a microprocessor to control all of these functions, and power supplies for the entire 5528A system (Fig. 3).

Since the 5528A measures relative motion or changes in position, not absolute distance, measurements are begun at arbitrary points along the axis of movement. That is, some arbitrary point is defined as zero for the measurement, and all future values are referenced to that zero. The **RESET** key on the 5508A front panel is used to define this zero point. Pressing **RESET** clears all measurement information and all error conditions. In some linear measurements the operator might want to define that arbitrary point as having some value, possibly to align the machine's scale with the 5508A reading. The **PRESET** key allows this. The operator can enter **12 PRESET** to label this starting point as 12 inches, for example.

Another example of the use of the preset feature is in velocity mode. An operator calibrating feed rate can preset a negative value equal to the desired velocity, and then try to drive the displayed velocity to zero. In straightness mode the **PRESET** key plays a different role. Here it is used to enter calibration numbers corresponding to the particular set of matched straightness optics being used. The 5508A uses this calibration data to adjust the straightness measurement accordingly.
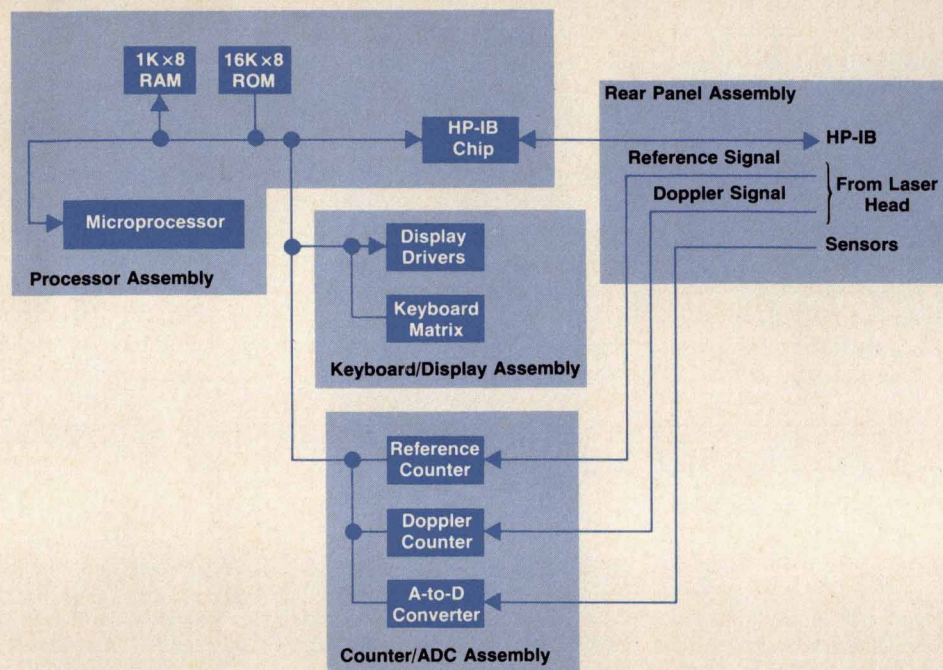
Fig. 3. *Block diagram of the 5508A Measurement Display.*

The **DIRECTION SENSE** key allows the user to change the polarity of the direction in which the optics bed is assumed to be traveling. If moving the machine in a particular direction yields increasing positive values, pressing the **DIRECTION SENSE** key causes the 5508A to change the readings to decreasing negative values. The direction of the data movement is mirrored around the PRESET value in linear and velocity modes. That is, if the zero point is 12 inches, and one inch of positive motion occurs, the 5508A will display 13 inches. Pressing the **DIRECTION SENSE** key reverses the sense of the measurement, but leaves the PRESET value alone. This yields a new distance value of 11 inches.

The **RESOLUTION** key allows the operator to choose how many decimal digits the display will show. The maximum allowed in linear measurements is six decimal digits in English units, corresponding to microinch resolution, and five digits in metric units, or 0.01-micrometer resolution. The operator might choose fewer digits to blank out the jittery least-significant digits in a high-vibration environment.

The last three measurement setup keys, **MATERIAL TEMPERATURE**, **V.O.L.**, and **EXPANSION COEFFICIENT**, are used in conjunction with atmospheric and material compensation (see box, page 12). They display the current values of these parameters, and in the case of manual compensation, they allow these values to be entered.

The keyboard also contains five mode keys, **LINEAR**, **VELOCITY**, **ANGLE**, **LONG STRAIGHTNESS**, and **SHORT STRAIGHTNESS**, which correspond to the five measurement types. Backlit keys indicate which type of measurement is being made. Any of the 5508A's front-panel keys, with the exception of **RESET**, can be exercised at any time without loss of measurement data.

The 5508A is equipped with the HP-IB for ease in data taking. It has full listener and limited talker capability. All front-panel functions can be programmed remotely over the HP-IB, and error conditions and display data can be read at any time. The **AUTO RECORD** key is used in conjunction with the HP-IB port. With it the operator can specify that the displayed data be sent over the HP-IB at regular time intervals. For example, pressing **2 AUTO RECORD** will send data every two seconds. This is convenient for logging data on external plotters, or for taking measurements on the fly.

Also supplied with the 5508A is a remote control unit that aids in optical alignment and data taking from up to 15 meters away from the 5508A. It contains a **RESET** key, a **RECORD** key for activating single HP-IB data transfers, and a beam strength meter for optical alignment purposes. It is especially convenient when used in conjunction with the 55288A Dimensional Metrology Analysis System (see box, page 4).

Fifteen different error messages can be displayed by the 5508A to aid the operator in diagnosing a problem in the measurement setup. Most errors do not result in loss of measurement data, but three errors related to the laser head or beam require the measurement to be reset.

Cumulative Frequency Counters

As mentioned earlier, the 5528A system measures optical path motions by counting the number of fringes or cycles incident upon the Doppler receiver and subtracting from this number the number of fringes or cycles incident upon the reference receiver. Each extra pulse the Doppler receiver sees over the reference (or conversely, each pulse the reference sees over the Doppler) corresponds to $\lambda/2$, or one-half of the laser wavelength, a distance of approximately 12 microinches. To see microinch movements, the system multiplies the two frequencies by sixteen before counting them, so that each counted pulse corresponds to $\lambda/32$, or about 0.78 microinch. The processor keeps track of the difference in counts in a software register called the software counter. The value in the software counter is di-

rectly proportional to the distance the optics have moved; the proportionality constant is $\lambda/32$. This relationship dictates that the 5508A counters cannot at any time fail to keep up with these incoming pulses, even when the counters are being read. It is this uninterruptable cumulative requirement that makes these counters unusual.

Fig. 4 shows a block diagram of the counter circuitry. The reference and the measurement channels are identical. First, for the purpose of extending the measurement resolution, the frequencies of the reference and Doppler signals are multiplied by 16. This makes it possible to measure fractional cycles of the original reference and Doppler signals by counting whole cycles of the multiplied frequency. The frequency multiplication is performed by a phase-

locked loop implemented on an HP semicustom integrated circuit.

An error detect block monitors the multiplier phase-locked loops. If the input frequency is too large or too small and approaches the tracking limits of the phase-locked loop, an error signal is generated. This indicates that the optics are slewing (moving) too fast. If the input goes away entirely, another error is generated, indicating the beam has been blocked so no light is returning to the receiver.

The multiplied reference and Doppler signals are sent to the pulse counters. These two independent channels are sixteen-bit synchronous counters, clocked by the incoming data stream. They generate a nonmaskable interrupt when the most-significant bit of either changes from a zero to a

Verifying the Laser Accuracy Specification

Verifying that the 5518A Laser Head meets its $\pm 1 \times 10^{-7}$ vacuum wavelength accuracy specification requires special equipment and techniques. A rule of thumb for calibration requires that the calibration technique have an error less than one-tenth that of the specification being tested. HP uses an iodine-stabilized helium-neon laser,[1] described below, as its wavelength standard. This laser has a vacuum wavelength error of less than 1×10^{-10} and the measurement technique adds no significant error.

The iodine-stabilized laser components are shown in Fig. 1. A standard helium-neon discharge tube contains the lasing medium. Two external mirrors form the resonant cavity. Varying the mirror spacing over a range of one-half wavelength tunes the output wavelength $\pm 4 \times 10^{-7}$ about line center. The iodine cell is inside the resonant cavity and affects the laser gain and output power as the wavelength changes. Each time the wavelength coincides with an absorption line in the cell, the output power changes slightly. The variation in output power is used to adjust the mirror spacing to make the laser wavelength coincide with the absorption line. These lines are very narrow because of the low pressure in the cell. Several lines occur within the $\pm 4 \times 10^{-7}$ tuning range. HP uses the line with wavelength 632.99123 nm recommended and measured by the U.S. National Bureau of Standards.

The measurement technique is also shown in Fig. 1. Rather than directly comparing wavelengths, which is quite difficult to an accuracy of 1×10^{-9}, the output frequencies of the iodine-stabilized laser and the 5518A under test are compared. The 5518A wavelength is then computed using an accurate number for c, the vacuum velocity of light (299,792,458 m/s). Because the

5518A emits light at two frequencies, a polarizer is used to select the vertically polarized one to match the polarization of the iodine-stabilized laser. The outputs of both lasers are then added using a 50% beam splitter and aligned to be coaxial. The resulting beam is detected by a high-speed photodiode and receiver. The receiver's output is the difference in optical frequency between the two lasers, typically 125 MHz. It is known that the standard's output frequency is greater than that of the 5518A, so the 5518A frequency equals the standard's frequency ($4.7361234039 \times 10^{14}$ Hz) minus the offset. The 5518A wavelength is then c ÷ (standard frequency − offset frequency).

Overall uncertainty is about 1×10^{-9}, including the values for c and the standard's output frequency.

Stability of the iodine-stabilized laser is better than 1×10^{-10}. Using the technique described above, many prototype lasers were measured to determine the nominal wavelength used by the 5508A Measurement Display (632.991393 nm). Typical 5518A stability of $\pm 1 \times 10^{-8}$ has also been measured. Production lasers are 100% tested to ensure that they meet the 1×10^{-7} specification.

Acknowledgment
I would like to thank Dr. Howard Layer of the U.S. National Bureau of Standards for his assistance in developing this test.

Reference
1. W.G. Schweitzer et al, "Description, Performance, and Wavelengths of Iodine Stabilized Lasers," Applied Optics, Vol. 12, page 2927, December 1973.
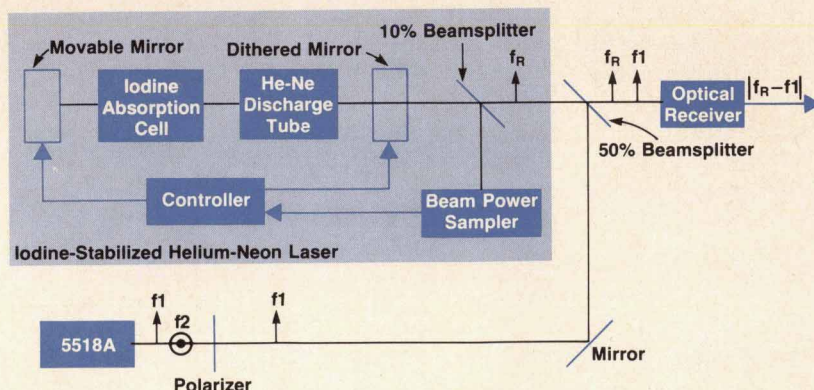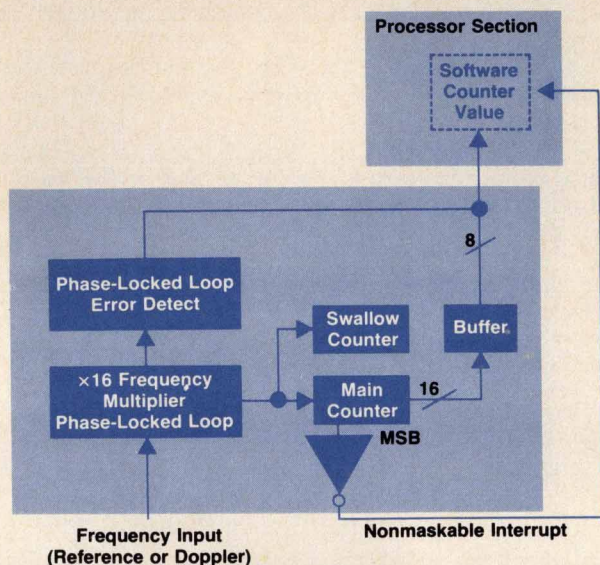
-Robert C. Quenelle

Fig. 1. Measurement technique for verifying the wavelength accuracy of the 5518A Laser Head.

Fig. 4. *Pulse counter block diagram. Multiplication of the input frequency by 16 increases the resolution so that each counted pulse corresponds to approximately 0.78 microinch in a distance measurement.*

one, that is, when either is half full. When this happens the microprocessor responds by reading the value of both counter channels. To avoid losing pulses during this reading operation, a pulse swallowing technique is used. The main counter value is frozen and the incoming pulses are diverted to a small swallow counter. This four-bit counter accepts the next sixteen incoming pulses, providing enough time for the main counter to be read by the microprocessor. After each swallow counter has seen sixteen pulses at its own counting frequency, its main counter is cleared and resumes counting. Note that both the reference and Doppler counters are halted for the same number of cycles, not necessarily for the same amount of time. The counts accumulated during this process need not

be taken into account because the software counter contains only the difference in counts.

Analog Subsystem

The analog-to-digital converter (ADC) subsystem in the 5508A transforms automatic compensation information (see box, page 12) into a form the microprocessor can use in its calculations. Fig. 5 shows the block diagram of this subsystem. Up to six external analog signals are used in compensation, three from the air sensor (temperature, pressure, humidity), and up to three from material temperature sensors. Fig. 5 shows these six inputs plus two more for analog ground and 0.5V, which are used during power-up self-testing. In normal operation each sensor outputs analog voltages between −1 and 1 volt. When no sensor is plugged into a particular channel, a resistor divider network floats the line at 2.5 volts. A comparator circuit checks for this condition, and if it exists, the microprocessor ignores that channel.

The analog-to-digital converter is a 12-bit dual-slope integrating ADC running at about five conversions per second. At the end of each conversion the ADC interrupts the microprocessor and the next conversion is begun. The reference voltage for the ADC is 0.5 volt, derived from a ten-volt, high-stability reference through a monolithic matched resistor divider. Instead of potentiometers with their vibration and drift characteristics, a digital calibration scheme is used. When the 5508A is returned to the calibration laboratory for its annual calibration, the 10V and 0.5V reference voltages are measured, and binary representations corresponding to their values are entered on a series of switches. These are read by the microprocessor, which then compensates for inaccuracies in these voltages in software. This design is very easy to calibrate and free from vibration and drift sensitivity.

Self-Tests and Diagnostics

Extensive self-tests and diagnostics are built into the 5508A and are exercised upon power-up. Immediately after
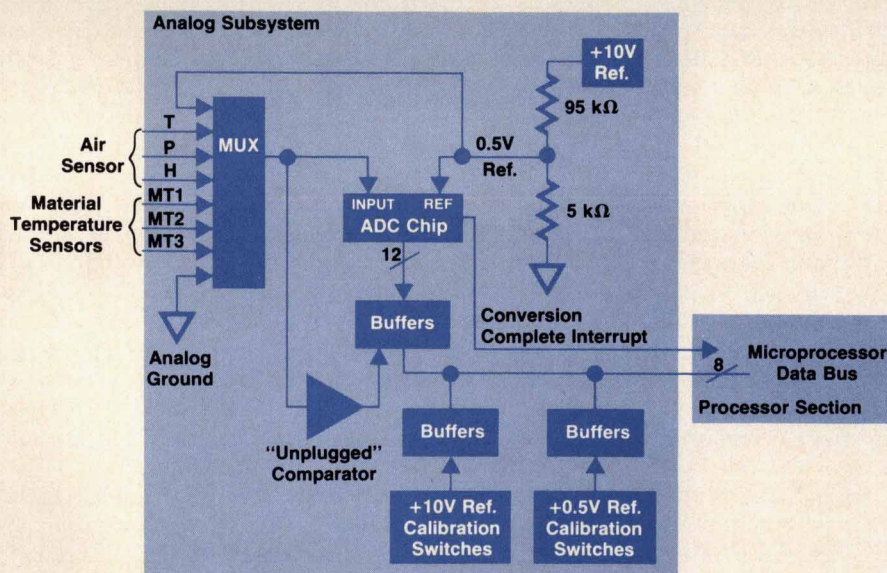
Fig. 5. *Analog-to-digital converter (ADC) block diagram. The ADC system transforms automatic compensation information into a form the microprocessor can use.*

Nonlinearity in Interferometer Measurements

The 5528A Laser Measurement System makes its various measurements by comparing the phase of the reference signal to that of the measurement signal. Each time the differential optical path in one of the interferometers changes by one wavelength, a phase shift of 360° occurs between the two signals. The 5508A Measurement Display uses phase-lock and statistical (averaging) techniques to resolve 10^{-5} mm, 10^{-6} inch, or 0.1 arc-second, depending on the measurement. While further resolution could be designed in, a subtle nonlinearity limits the usefulness of such efforts.

The nonlinearity is periodic, with a period of one wavelength optical path change. It is a result of not perfectly separating the optical components, f1 and f2, into the two arms of the interferometer. The nonlinearity occurs solely as a result of optical leakage and is not a result of any technique used to resolve fractional wavelengths.

Leakage of the wrong optical component into an arm of an interferometer occurs for several reasons. The light leaving the 5518A is not perfectly linearly polarized, being instead slightly elliptically polarized. Further, the alignment perpendicular and parallel to the mounting feet is not perfect. The optics themselves are not perfect and angular misalignment between the 5518A and the interferometer optics causes leakage. Manufacturing tolerances and adjustments are designed to control all these effects to an acceptably small level.

Fig. 1 shows a computed error plot of nonlinearity versus optical path length change for worst-case conditions. The peak-to-peak phase error is 5.4°, corresponding to 4.8×10^{-6} mm (0.19×10^{-7} in) in distance mode and 0.03 arc-second in angle mode. Both these errors are much smaller than the respective resolution limits. The errors for short- and long-range straightness are 1.7×10^{-4} mm (6.2×10^{-6} in) and 1.7×10^{-3} mm (6.2×10^{-5} in), respectively. The errors for straightness are larger because of the nature of the interferometer.

Since the nonlinearity error is so small, it is virtually impossible to measure directly. Instead, a model incorporating the elliptical polarization, misalignments, and optical imperfections was developed to predict the nonlinearity error. The model was then used to determine levels for the various errors consistent with the desired system performance.

Nonlinearity caused by optical leakage affects all interferometers, whether single-frequency or two-frequency. In the case of the 5528A, the nonlinearity error is typically much smaller than other limitations occurring during measurements. This error does set a limit on the ultimate resolution of the interferometer and is included where appropriate in the specifications.
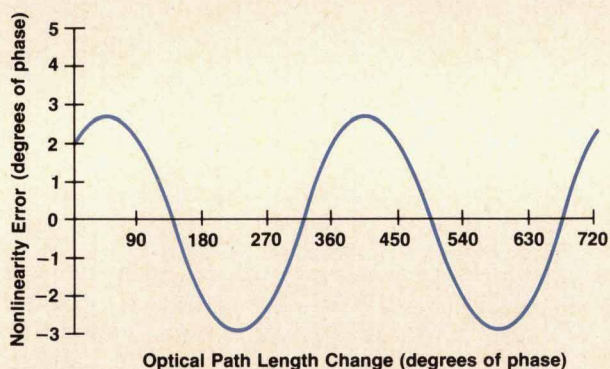
-*Robert C. Quenelle*

Fig. 1. *Worst-case errors resulting from imperfect separation of the two beam components.*

power is applied, the 5508A performs a checkerboard RAM test, followed by a ROM checksum. The checksum routine is arranged as a sort of signature analysis algorithm, using a feedback shift register technique. This test is performed on the contents of the 16K program ROM. If the RAM or ROM fails its test, an error message is displayed and the 5508A is locked out, that is, the operator is unable to make a measurement until the problem is fixed. If the 5508A passes this test, it begins testing the counters.

The first counter test begins by defeating the reference frequency from the laser head and switching the microprocessor's 1-MHz clock into the reference channel's phase-locked loops. The counter is cleared and a short time delay is generated in software. During this time an exactly known number of counts should accumulate in the reference channel if all is working properly. Since the clock signal being counted is the same signal that is used to generate the software time delay, the exact frequency of the clock is not critical; a delay equal to a particular number of system clock cycles should always produce the same number of pulses counted. A second time delay is then generated, yielding another value in the counters, this one the binary complement of the first. Thus both binary states in each bit of the reference channel counter are checked. If

the 5508A passes this test, the message PASS 1 is displayed. A failure produces the message FAIL 1 and the 5508A cannot be configured for a measurement until the problem is fixed.

The second counter test is exactly like the first, except that the measurement channel of the counter is verified, rather than the reference channel. Either PASS 2 or FAIL 2 is displayed.

The third self-test involves the counters in free-running mode. Once again the microprocessor system clock is used as the counter inputs, emulating the laser source's reference and Doppler signals. The counters are allowed to run free for a longer delay, during which time they interrupt 150 times. Since both channels have the same input (the system clock), they should always have the same number of counts, plus or minus one for jitter. If they do not interrupt 150 times in 0.5 second, or if there is a net number of counts (i.e., one channel is counting more than the other), the message FAIL 3 appears. Once again this means the 5508A must be repaired before a measurement can be taken.

The last self-test on power-up involves the ADC. During this test the ground signal and the 0.5V reference signal are converted to digital form and read. The ADC is a ratiometric device, so the exact value of the 0.5V reference doesn't

matter; the test only checks the activity of the ADC and the existence of the reference. After the conversions there is a time delay to wait for the ADC to interrupt at least once. This exercises the interrupt control circuitry. If either of the two conversions fails to agree with predetermined values, or if the ADC doesn't generate an interrupt in the time allotted, then the unit displays FAIL 4. Otherwise it shows PASS 4 and goes on.

The 5508A then displays the values of the two digital calibration switches, one for the 10V reference and the other for the 0.5V reference, before beginning the laser head warmup sequence.

Laser Head

The 5518A contains a helium-neon laser that lases at only a single wavelength (single spatial and temporal modes). This single frequency is split into two discrete frequencies by applying an axial magnetic field to the laser. The field causes the lasing atoms to emit left-hand circularly polarized light at one frequency and right-hand circularly polarized light at a second frequency (f1 and f2 in the measurement theory discussion). Birefringent mica plates are used to convert the circular polarizations into two linear components, one perpendicular and one parallel to the mounting feet.

If not tuned, the laser can emit light varying in frequency about 2.5 ppm (1.2 GHz) as the laser mirror spacing varies by one-half wavelength. The difference frequency is only usable in the region ±0.3 ppm around the center frequency (line center), so a control scheme is needed to maintain cavity length. The cavity length is in fact controlled to better than ±0.3 ppm, making more accurate measurements possible.

As the cavity length changes, the laser output power cycles. The output from each polarization peaks at a different cavity length. Fig. 6 shows a plot of the difference in
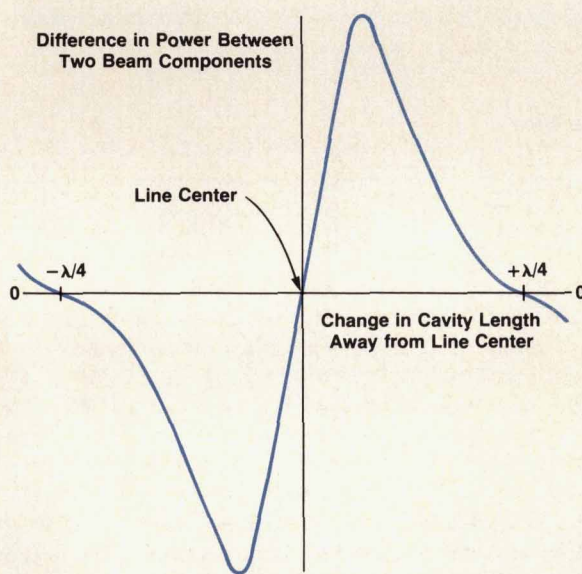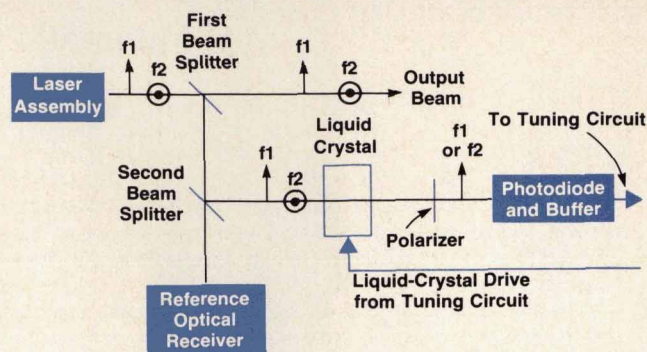
Fig. 7. Beam sampler takes accurate samples of the two beam components so that the microprocessor can generate a turning error voltage for controlling the laser cavity length. Cavity length is varied by heating a glass rod.

power between the two components versus cavity length. Note the zero crossings that occur per cycle, indicating points where both components have equal power. Line center occurs at the zero crossing on the steeper slope. The powers are equal at line center because the magnetic field splits the two frequencies symmetrically away from where line center would be with no field applied.

The laser output frequency is also affected by the gas pressure and composition. The laser tubes are filled automatically to get repeatable performance.

Earlier HP lasers used a polarizing beam splitter and two matched photodiodes, one for each beam component, to generate the tuning curve. The 5518A is designed to eliminate the alignment and matching requirements of the earlier design. The beam is now sampled by a pair of beam splitters arranged to cancel preferential reflection of f1 or f2, thus ensuring an accurate beam sample. Fig. 7 shows the beam sampler operation. A liquid-crystal cell passes f1 and f2 unaltered when on or rotates the polarization of each 90° when off. The polarizer passes only the vertical component, either f1 or f2, depending on the state of the liquid crystal. The control circuit synchronously switches a subtracting sample-and-hold circuit and the liquid crystal to generate the tuning error voltage for controlling the cavity length.

The 5518A also uses a new means of adjusting cavity length. In previous designs, the laser mirrors were separated by a rod made of very low-thermal-expansion material and minor length correction was accomplished with a piezoelectric crystal. Thermal tuning produces a more economical laser. The 5518A uses an ordinary glass rod whose length is controlled by varying its temperature with a heater wire wrapped around it. Since the heater can only raise the temperature of the rod, a preheat cycle is required to ensure that the rod can always cool by losing heat to its surroundings. During preheating, the rod is quickly heated to a temperature known to exceed the temperature it would reach if the laser were left on indefinitely at 40°C without heater power. The heater wire itself is used to measure rod temperature by occasionally turning off the heater, letting the wire cool to the rod temperature and measuring its resistance.

Although the new tube is simpler than the old one, the dynamic response of the heated rod is more complex than

Fig. 6. HP's two-frequency laser produces light beams consisting of two components that differ in polarization and frequency. As the laser cavity length changes, the power in each component peaks at a different length.

Automatic Compensation

by Deane A. Gardner

The 5528A Laser Measurement System measures distances in terms of wavelengths of helium-neon laser light. In vacuum, this wavelength is a fixed constant of nature, allowing very high measurement precision.

In an atmosphere, which is always present in machine shops and metrology laboratories, the refractive index of air shifts the laser wavelength, producing a scale factor error. This local refractive index varies nonlinearly with temperature, pressure, and relative humidity according to an empirically determined formula:[1]

$$N = 1 + (9.74443 \times 10^{-6}\, P)\, \frac{1 + 10^{-6}\, P(26.7 - 0.187T)}{0.934915 + 0.0020388T}$$

$$- 1.089 \times 10^{-3}\, Re^{0.0325T}$$

where P is atmospheric pressure in inches of mercury, T is temperature in degrees Fahrenheit, R is relative humidity in percent, and N is the calculated refractive index. The 5508A Measurement Display evaluates a simplified version of this equation, using information supplied by the 10751A Air Sensor, to give a compensated system accuracy of 1.5 parts per million.

The 10751A Air Sensor is the system weather station. It continuously furnishes data on air pressure, temperature, and humidity to the 5508A. Pressure is measured with a bridge-type strain gauge transducer derived from standard aerospace components. Microvolt changes in the output of the strain gauge are amplified by an autozero amplifier in the 10751A, giving a stable pressure reading accurate to 1.5 millimeters of mercury at room temperature.

Air temperature is determined with an integrated circuit current-source-type sensor. The sensor's output current is converted to a dc voltage by an operational amplifier, providing the 5508A with temperature information accurate to 0.4°C.

The effect of relative humidity on the refractive index of air is fairly minor, and humidity sensors with electrical outputs are very expensive. For these reasons, a three-position humidity switch is included on the air sensor in lieu of a costly transducer. The operator just sets the switch to approximate ambient conditions,
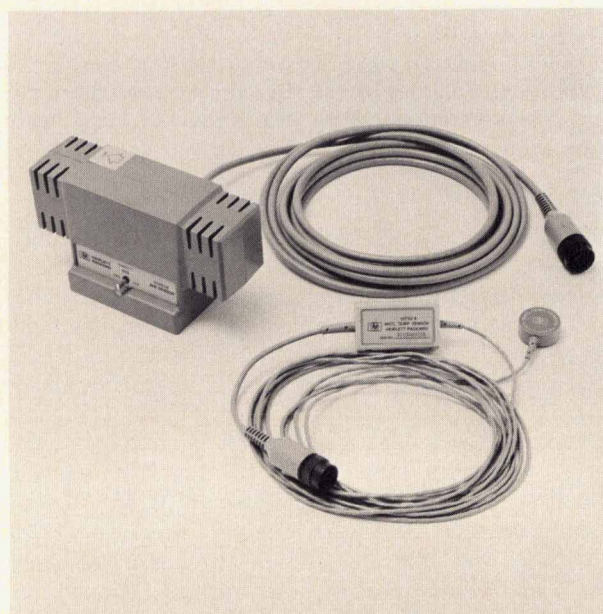

Fig. 1. *10751A Air Sensor (upper left) and 10752A Material Temperature Sensor (lower right).*

selecting one of three voltages to be fed back to the 5508A calibrator control unit.

The 5528A can also correct for material expansion with temperature. The 10752A Material Temperature Sensor, a small button attached magnetically to the workpiece, sends machine tool temperature information back to the 5508A in a manner similar to that of the 10751A Air Sensor. Once the material's temperature coefficient of expansion is entered, the 5508A computes expansion effects and normalizes all measurements to 20°C.

Fig. 1 shows the 10571A and 10572A Sensors.

Reference
1. B. Edlén, "The Refractive Index of Air," Metrologia, Vol. 2., no. 2, 1966, p. 71.

that of the piezoelectric crystal. Heat flow is three-dimensional and distributed. The dynamic response was measured and then modeled. The transfer function for length change per watt includes a simple pole at about 1 mHz (the period of 1 mHz is about 17 minutes), followed by additional phase shift that begins accumulating at about 100 mHz, reaches 180° at 1 Hz and increases indefinitely above 1 Hz. Large-signal response is further complicated because heat can be added faster than it can be lost, resulting in asymmetrical slew rates. The controller contains an integrator for zero steady-state length error, a zero which approximately cancels the 1-mHz pole, and a lead-lag network which slightly improves transient response. The controller also contains a diode network to square the heater feedback voltage, which makes the loop gain constant for power, the controlled parameter.

When the 5518A is switched on, the controller first preheats the rod as described above. After a few minutes, when the rod is warm and the power level has stabilized, the controller switches to optical feedback derived from the beam sampler. The cavity length is then adjusted to be a multiple of one-half wavelength at line center. Cavity length is typically controlled to keep the output wavelength stable to 0.01 ppm, corresponding to a length change of about 1.27 nm (5×10^{-8} in), or an average rod temperature change of only 0.003°C (0.0055°F). The average rod temperature is maintained although the temperature distribution in the rod varies considerably during warmup and at different operating temperatures.

The two optical receivers in the 5518A consist of a polarizer, a photodiode, a semicustom HP integrated circuit and passive components. The two coaxial beams, f1 and f2,

are orthogonally polarized and don't interfere. The polarizer is used to project both beams into a common axis halfway between the original axes so that they do interfere. The photodiode converts the resulting intensity variations into a current. The current, which ranges in frequency from 0.5 to 3 MHz and in amplitude from 5 to 100 microamperes, is amplified, limited and converted to TTL levels by the semicustom IC. The IC also provides a dc signal proportional to optical signal strength (used to drive the beam strength meter), LED drive signals, and automatic signal gating based on signal level.

Acknowledgments

The initial design work on the 5508A processor section and software was done by Perry Jeung. Gerry Lazzareschi designed the special counters, and John Beckwith designed the semicustom phase-locked loop IC for those counters. Jim Hutchison worked on the design of the analog subsystem, the 5508A power supplies, and the 10751A and 10752A Sensors. Mike Munrow supported the 10751A and 10752A and developed a production calibration system for them. Al Low did the mechanical design of the 5508A. R&D management guidance was supplied by Hans Wiggers and lab managers Skip Ross and Webb McKinney. Dennis Kwan had the responsibility of bringing the 5508A into production. The 10751A and 10752A Sensors were supported in production by Tim Petersen. Production engineering managers Pierre Patkay and Bruce Corya and manufacturing managers Pete Moseley and Dan Bechtel supported the 5528A throughout its design and production. The semicustom photodetector amplifier IC in the 5518A was designed by Tom Jochum. Russ Loughridge worked on introducing the 5518A into production. Several people in marketing contributed greatly to the initial definition and documentation of the product. Special acknowledgment should be given to Alan Field and Rod Dinkins for their contributions to the serviceability of the 5528A, and to Tim Kelly, Bob Perdriau, and John Buck for their extra effort in generating the user documentation. Bruce Euler and Art Weigel in the quality assurance department, Conrad Levine and Wayne Egan in environmental test, and Steve Leitner and Andy Dickson in regulations engineering helped ensure that the 5528A meets its ambitious quality goals. Materials Engineers Steve Kong, Terry Bowman, Sandi Ordinario, Nick Nichol, Dave Moncrief, Bill Anson, and Bill Jeans helped qualify key components and vendors and analyzed failures to improve the design. Glenn Herreman and Cecil Dowdy

provided excellent inputs regarding the 5528A's ease of use and features during its development.

References
1. Hewlett-Packard Journal, Vol. 21, no. 12, August 1970.
2. R.R. Baldwin, G.B. Gordon, and A.F. Rudé, "Remote Laser Interferometry," Hewlett-Packard Journal, Vol. 23, no. 4, December 1971.
3. R.R. Baldwin, B.E. Grote, and D.A. Harland, "A Laser Interferometer That Measures Straightness of Travel," Hewlett-Packard Journal, Vol. 25, no. 5, January 1974.

Deane A. Gardner
Deane Gardner joined HP in 1980 and the following year assumed responsibility for the 10751A Air Sensor and the 10752A Material Temperature Sensor. He also designed electronics and mechanical tools for the 5528A Laser Measurement System's analog electronics. A 1980 graduate of the California Institute of Technology, he holds a BSEE degree, hails from Los Angeles, California, and now lives in San Jose, California. He likes racquetball, volleyball, and skiing and is restoring his 1969 Firebird convertible.
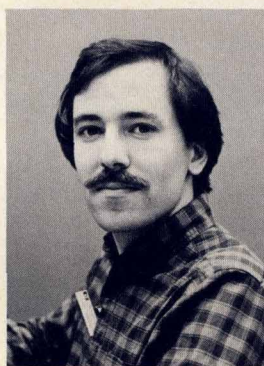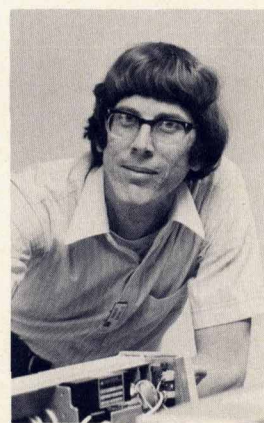
Lawrence J. Wuerz
Larry Wuerz is a native of St. Louis, Missouri and a graduate of the University of Missouri at Rolla. He received his BSEE degree in 1978 and joined HP in 1979 as a development engineer for the 5508A Measurement Display. Later he became project manager for all of the electronics and software in the 5528A Laser Measurement System. In 1982 he received his MSEE from Stanford University. Married to a HP engineer, Larry lives in Santa Clara, California, enjoys camping and home computers, and plays softball and golf.
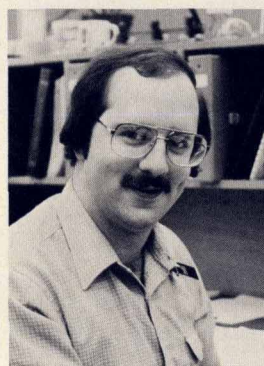
Robert C. Quenelle
Bob Quenelle has been a design engineer with HP's Santa Clara Division since 1973. He designed the 545A Logic Probe and wrote system software for the 5046A Digital IC Test System before joining the 5528A Laser Measurement System project team as one of its first members. Born in Tucson, Arizona, he attended the University of Arizona, graduating in 1970 with a BSEE degree. In 1973 he received his MSEE degree from Stanford University. He is married, has a daughter, and lives in San Jose, California. Bob's interests include radio controlled boats, playing guitar, and family outings.

Christopher Burns
Chris Burns joined HP in 1979 after receiving his BSEE degree from Rice University. He served as a production engineer for digital signal analysis and laser measurement products, then joined the laser R&D laboratory in the later stages of the 5528A project. A native of San Antonio, Texas, he now lives in San Jose, California and enjoys outdoor sports and reading.

Laser Optical Components for Machine Tool and Other Calibrations

by Richard R. Baldwin, Larry E. Truhe, and David C. Woodruff

IDEALLY, A MACHINE TOOL CALIBRATION device should be capable of completely describing the motion of a rigid body such as a machine tool slide. This requires six independent measurements, since any moving object has six degrees of freedom of motion: it can translate in three orthogonal directions and rotate about three orthogonal axes (see Fig. 1). In machine tool language, the unwanted motions corresponding to these six degrees of freedom are called positioning error, horizontal positioning error, vertical positioning error, pitch, yaw, and roll.

The relative importance of these unwanted motions depends on the type of machine tool in question. For example, a properly designed single-axis measuring machine requires good positioning accuracy, but need not be free of angular motion. A tracer lathe, however, must be free of angular motion, but has no "positioning accuracy." It has no position sensing transducer at all; it simply follows a template. Surface grinders require good straightness and must be free of roll, but can tolerate pitch and yaw so long as straightness is not affected (see Fig. 2).

There are, of course, many machine tools of a more complex nature, such as the coordinate measuring machine and the N/C (numerically controlled) mill, that are adversely affected by any unwanted motion. For these machines all six degrees of freedom are more or less equally important. It is interesting that the more complex machines are not only the most difficult to calibrate, but are also generally less accurate than the simpler types.

The HP 5528A Laser Measurement System is capable of measuring five of the six degrees of freedom, the exception being roll. It can also measure related parameters such as flatness, squareness, and parallellism. This is accomplished through the use of optical accessories, or inter-
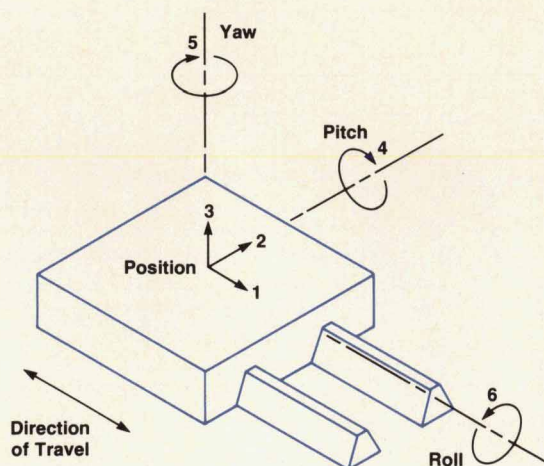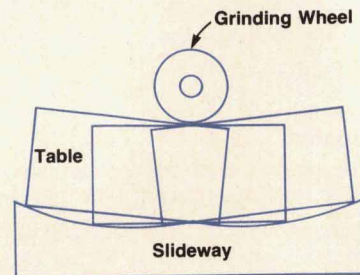

Fig. 2. *A surface grinder table shown in three positions on a way. This type of motion results in angular pitch but does not affect the straightness of a ground part.*

ferometers, each of which has been specifically designed to measure a particular degree of freedom.

The Linear Interferometer

The three basic interferometers offered as part of the 5528A system are linear, angular, and straightness interferometers. The HP 10766A Linear Interferometer (Fig. 3) is the simplest of the three. It is similar to the interferometer used by A.A. Michelson in the 1890s to measure the length of the meter. Its principal advantage over Michelson's is that it uses cube corner retroreflectors instead of plane mirrors. Since a cube corner reflects any incident light ray exactly parallel to its incoming direction, the cube corner requires no angular adjustment. The linear interferometer uses many of the same optical components as the previous system's remote interferometer,[1] but is smaller, lighter, and does not require precise lapped surfaces since it is used only for linear measurement. The linear interferometer is only 40 mm on a side and can be fixtured for almost any application.

Angular Optics

The angular interferometer, which was previously offered as an add-on for the remote interferometer,[1] has been redesigned as a separate accessory. Since the requirements for linear and angular measurements are different, it is more cost-effective to offer two interferometers rather than a single interferometer that can do both kinds of measurements. The linear interferometer should be small and easy to use, but the accuracy of the measurement depends not on the interferometer but on the laser, so there is no need for close mechanical tolerances. This is not true of the angle interferometer. Here the accuracy of the measurement depends primarily on the interferometer. The HP 10770A Angular Interferometer (Fig. 4) consists of a rhomboid beamsplitter, which causes the two interfering laser beams to come out parallel to each other, and two cube corner reflectors attached to a common mount. If the reflector mount were to rotate about an axis perpendicular to the plane of
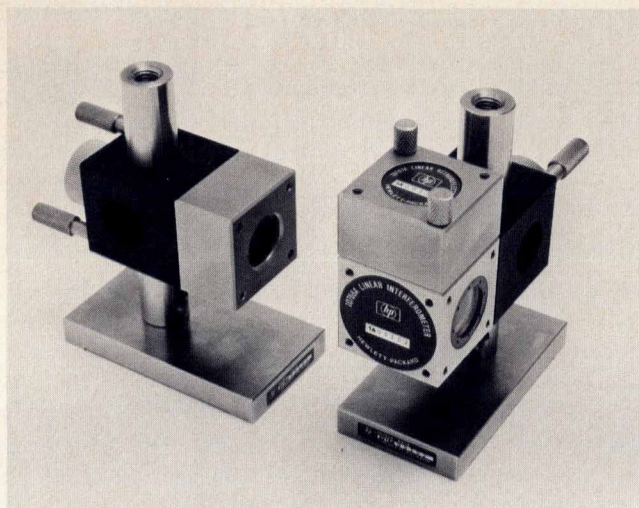

Fig. 1. *Six possible unwanted motions of a machine tool slide.*

Fig. 3. HP 10766A Linear Interferometer.

the figure, the interferometer would measure the distance x, which is given by

$$x = S\sin\theta$$

where S is the separation between the nodal points of the cube corners and θ is the angle of rotation (see Fig. 5). If the angular rotation θ is small, which is generally true of machine tool pitch or yaw, then one can assume that $\sin\theta = \theta$ and $x = S\theta$.

The accuracy of the angular measurement is directly proportional to the accuracy of the cube corner spacing S. This imposes tight tolerances on cube corner location. The cube corner spacing error in the new angular interferometer causes only 0.2% error in the displayed measurement.

It is also important that the two interfering beams leaving the angular interferometer be precisely parallel. If they are not, two problems result. The first and most obvious problem is that it is impossible to align both beams parallel to the reflector travel unless the two beams are themselves paral-
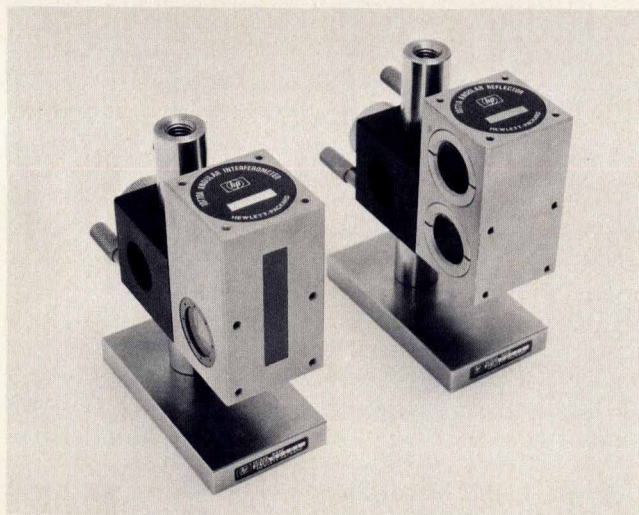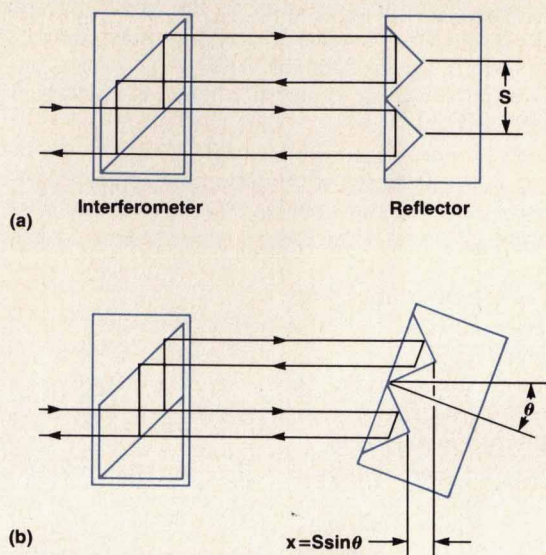

Fig. 4. HP 10770A Angular Interferometer.

Fig. 5. Optical schematic of the angle interferometer. In (a) both beams travel the same distance from the interferometer to the reflector. In (b) the paths differ by the amount x because of rotation of the reflector. For small θ, $\theta = x/S$.

lel. Nonparallelism causes one or both beams to move away from the cube corner reflectors as the reflector mount is moved away from the interferometer. Eventually the beams become so misaligned that it is impossible to make a measurement.

The second and less obvious problem is that poor beam parallelism can cause an error in the measurement. This results from what is commonly referred to as cosine error. This error results from the fact that the interferometer measures only the component of reflector motion that lies in the direction of the laser beam. The effect of this on angular measurement is shown in Fig. 6 which illustrates an apparent pitch ϕ resulting from beam nonparallelism. In this case the angular reflector moves through a distance D. The lower
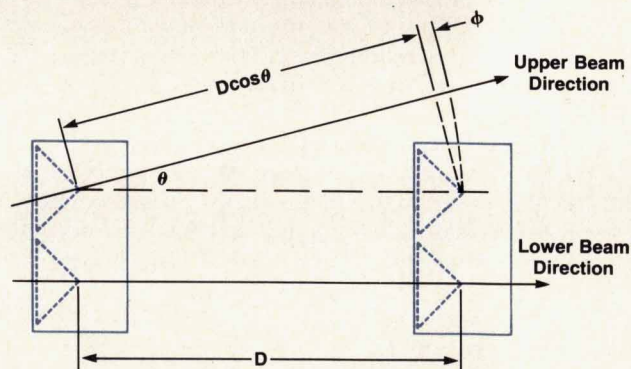

Fig. 6. Apparent pitch ϕ resulting from laser beam nonparallelism. Although the full distance traveled (D) lies along the lower beam, only the component $D\cos\theta$ lies along the upper beam.

laser beam, which is parallel to the travel, increases in length by the full distance D, but the upper beam only increases along the component $D\cos\theta$. This causes the interferometer to read an apparent pitch ϕ even though none actually exists.

Beam parallelism in the angular interferometer is determined by the accuracy of the rhomboid beamsplitter and is held to a tolerance that ensures that the apparent pitch error does not exceed 0.05 arc seconds per meter of travel.

Straightness Optics

The straightness interferometer offered with the 5528A System is essentially the same as that offered with the earlier 5526A System.[2] However, it is offered with more fixturing and the straightness reflector has been made smaller for ease of use.

The principal advantage of the new system for straightness measurement is increased convenience. The whole system has been designed with straightness in mind. It is no longer necessary to add an external resolution extender to adapt the system to straightness. Long- or short-range straightness measurements can be made by simply pushing a button on the 5508A Measurement Display and setting the turret on the 5518A Laser Head to the straightness position.

Ease-of-Use Considerations

Ease of use was an early design consideration for the 5528A Laser Measurement System. A major drawback in using previous laser interferometers has been the amount of time required to complete the initial alignment procedure and the inconvenience of having to repeat it all over again when going from one type of measurement to another (e.g., linear to angular or angular to straightness). The 5528A optics are designed to minimize setup times and reduce the number of alignments.

A key concept in the design of all components is the common centerline approach. The goal is to have the operator do one initial alignment of the 5518A Laser Head on a given machine tool. After that is accomplished, all fixtures and optical components are interchangeable on universal mounts. The common centerline approach requires that the laser beam be aligned parallel to one axis of the machine and positioned 105 mm above the machine bed. To aid the operator, several alignment targets (discussed later) attach to the optics housings.

Post, Height Adjuster, and Base

The 55280A Linear Measurement Kit includes two 10784A Bases and three 10785A Post and Height Adjuster assemblies. This combination provides the user with sufficient fixturing to accommodate most measurement applications.

These parts are designed to offer flexibility in positioning the optics along with highly rigid structures to ensure stability during measurements. The post can be inserted into any of four sides of the height adjuster, and the attached optics can then be quickly rotated through any 90° interval. A large thumb knob secures the height adjuster to the post at any desired height and 90° rotation position. The thumb knob can be easily removed and the post inserted into the threaded hole that held the knob. This allows the post to be chucked into a standard lathe or milling machine collet, thereby expanding its range of applications.

The 30-mm-square bolt pattern used for mounting optics to the height adjuster is universal for the 5528A System optics and fixtures. Two captive thumbscrews are provided. The captive screws contain knurled portions that extend beyond the large height adjustment knob for convenient hand tightening.

The post and base are constructed of durable stainless steel. The base is precision-ground to ensure accurate vertical positioning of the post when assembled. A cross hole is provided in the post so that a screwdriver shank or rod can be inserted for tightening the post. The underside of the base is relieved in the center, leaving two parallel pads at opposite ends of the base. This minimizes problems with small burrs or other irregularities in a machine bed causing the base to mount unevenly. The base can be secured to the machine bed using standard clamps.

With the height adjuster mounted on the post in the uppermost position, the attached optics are automatically at the 105-mm common centerline height. Once aligned, system optics can be interchanged, depending on the type of measurement desired, without having to go through realignment procedures each time.

Leveling Plate Mount for Turning Mirror

The 10772A Turning Mirror includes a leveling plate mount which greatly eases its alignment during setup.

The leveling plate is a low-profile unit consisting of a base with an attached pivoting two-axis platform into which the turning mirror or other optics can be mounted. The base in turn can be mounted directly to a 10785A Post, 10777A Optical Square, or 10785A Height Adjuster by using the standard shaft included with the kit.

Two knurled thumb knobs provide a convenient two-axis adjustment for any attached optic. The adjustment range for each axis is ±6°.

The turning mirror consists of a highly reflective mirror mounted at a fixed 45° angle in a stainless-steel housing. Two captive screws are included for attaching it to the leveling plate or any other appropriate system component.

Straightness Accessory Kit

The 10776A Straightness Accessory Kit contains a large 63-mm-diameter retroreflector, a reflector mount for the 10774A/75A Straightness Reflector, and mounting hardware and ports for the straightness interferometer. The reflector mount greatly simplifies straightness setup operations. Two micrometer adjustment screws are built into a two-axis positioning platform, and a 360° pivot mechanism with 90° detent stops is built into the adjustable platform. This combination provides a wide range of alignment positions for the attached optics.

With this accessory kit, straightness measurements can be made in both horizontal and vertical axes. Because of the reflector mirror pivot capability, any optical straightedge inaccuracies can be eliminated by rotating the mirror 180° and repeating the measurement.

All components have been designed to mount in a number of orientations and combinations to lend themselves to a wide range of applications. Captive screws are

Manufacturing the Laser Tube

by Richard H. Grote

A concept that has recently become widely accepted in manufacturing circles is that producing a high-quality product is a matter of adequately controlling its manufacturing process. This means that the manufacturing process must be designed to ensure that every product is manufactured in exactly the same way. This concept is particularly significant in building a very high-technology product such as a HeNe laser. Early in the development of the thermally tuned 5518A laser tube it was decided to make the necessary investment in manufacturing equipment to ensure that the process would be under control.

The laser tube was designed to operate in the lowest-order transverse mode, TEM_{00}. The laser capillary rod has a stepped bore diameter that suppresses higher-order modes and optimizes output power. It is very important that the two bore holes are accurately drilled and concentric. Eccentricity of these two bores can seriously degrade laser tube power. The rod is drilled with a custom-designed five-spindle core drilling and grinding machine (see Fig. 1). It core drills the capillary holes simultaneously from both ends, then grinds a concave shape into the end of the rod, and finally convex-bevels the rod end. It is capable of producing very uniform parts with one setup and six cutting functions, replacing 27 manual operations on two machines.

The laser cavity length is tuned by means of current flowing through a heater wire wrapped around the capillary rod to control the temperature and hence length of the rod. Failure to wrap the heater wire uniformly and tightly results in a heat transfer characteristic that varies from one laser tube to another. A machine was designed and built to wind wire precisely at a defined tension into grooves cut into the rod. Before the machine was invented, the wire was wound by hand. One can see in Fig. 2 the improvement in heat transfer uniformity provided by the wire winding machine.

Probably the most important components of a laser tube are the laser mirrors. Mirrors with out-of-tolerance reflectance or poor surface quality can produce a low-power laser or no laser at all. To manufacture high-quality laser mirrors as well as other optical
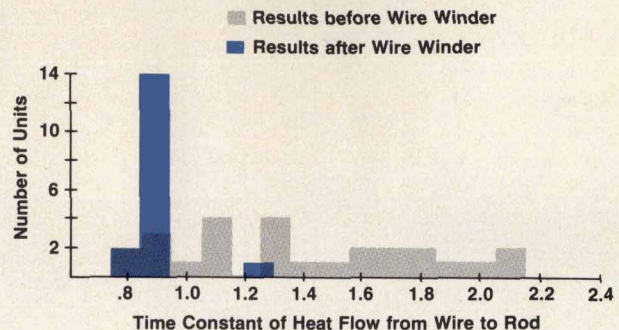
Fig. 2. *Improvement in heat transfer uniformity provided by the specially designed wire winding machine.*

components of the 5528A laser system, a new optical coater was purchased. This coater deposits thin-film dielectric materials on glass substances to produce highly reflective, antireflective, and other coatings. It operates as a turnkey system. Once substrates are loaded into the coater chamber, vacuum bakeout, substrate temperature, material deposition rates, and film thickness are under computer control. This is a major departure from the classical manual coating operation and has resulted in much greater uniformity from one coating run to another. Once laser mirrors have been coated, it still is an onerous job to measure all of their optical characteristics manually. Another special computer-controlled machine was constructed that measures reflectance, transmittance, forward scatter, and backscatter and calculates absorption of the mirrors.

One additional key to good laser operation is the purity of the HeNe mixture. Impurities in the tube can cause the laser to have low power, high noise levels, and shorter lifetime. Consequently, very good vacuum practices are necessary to ensure that all residual gases are removed from the laser tube before it is filled
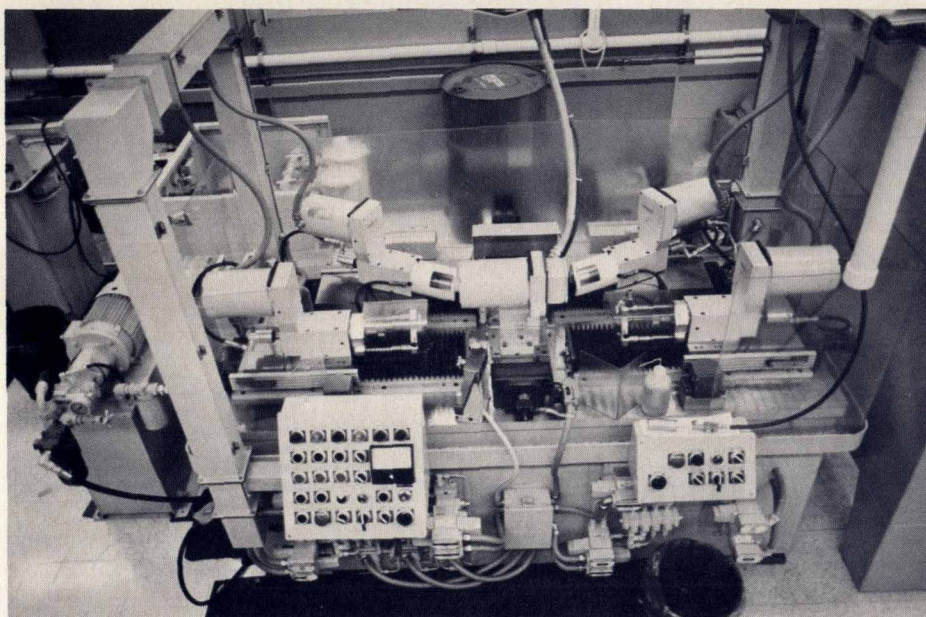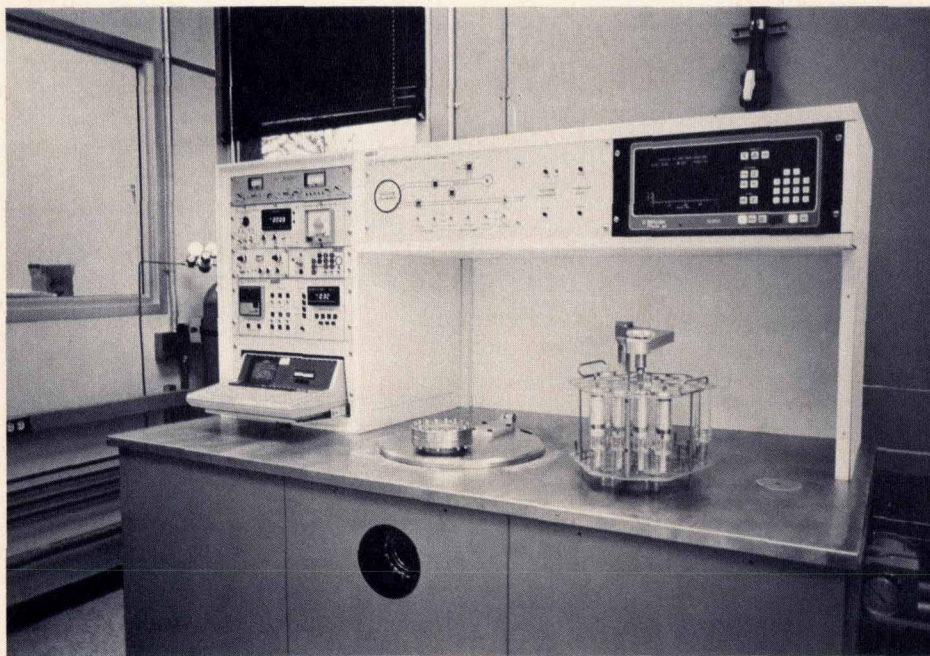
Fig. 1. *Custom-designed five-spindle core drilling and grinding machine.*

Fig. 3. *Custom-designed machine bakes out, fills, and seals laser tubes.*

with its HeNe mixture. Yet another custom machine was built to vacuum bakeout the tube, fill it, and seal it (see Fig. 3). The entire processing operation is automatic. An operator loads tubes into the processing station, starts the HP-85 control program, and walks away. Later, completely filled and sealed laser tubes are removed from the station ready to test. The HP-85 Computer monitors important process parameters and prints out a permanent record. The laser tube processing station provides tubes that are much more uniform with much less human effort than was necessary in the older, manual processing approach.

This heavy investment in manufacturing equipment allows much better control of the process of building laser tubes. For those process steps that are not automated, clear and precise documentation is necessary to tell the people building the laser exactly what to do at every stage of manufacture. Nearly sixty separate process sheets have been written, documenting all of these operations. The combination of well documented processes and automation has resulted in a very well controlled laser tube manufacturing process.

Acknowledgments

Ernie Riberdy designed, specified, and brought on-line the rod drilling machine. He also designed and constructed the wire winder. Jeff Benzing and John Tsai specified the optical coater and made it operational. Jeff also designed and built the laser processing station. Dave Woodruff designed and constructed the mirror tester.
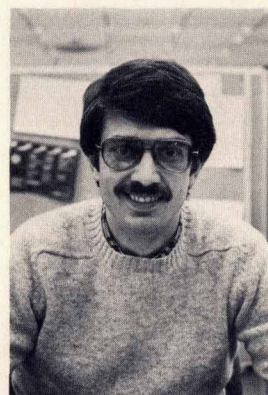
Richard H. Grote
Dick Grote was born in Indianapolis, Indiana. He received his BSEE degree from the University of Kansas in 1969 and his MSEE from Stanford University in 1971. After joining HP in 1969, he spent 9½ years in digital signal analysis R&D, then three years in manufacturing, the last two as production manager for laser interferometer products. He became project manager for the 5518A Laser Head last year. Dick, his wife (a former HP engineer and HP Journal author), and their two small daughters live in Palo Alto, California. Among his leisure activities he lists reading, music, and coping with two children in diapers and a balky sprinkler system.

included for convenience in attaching the reflector mirror.

Optical Square Mount

The 10777A Optical Square is an indispensable tool for measuring the perpendicularity between major machine tool axes. To avoid cosine errors caused by misalignment of the optical square to the machine axis, a suitable mounting platform is required. While some measurements benefit from a stand-alone optical square, most measurements can accommodate the extra space required for an auxiliary mount that improves the accuracy and speed of setups for machine tool calibrations.

By itself, when used in the flat or horizontal position, the optical square can be located very accurately on its three built-in precision-ground footpads. However, this position does not satisfy the common centerline criterion of the system. In the vertical position, the square has a narrow base which makes it difficult to position with the perpendicular accuracy needed, and because of its relatively large volume, it is awkward to clamp or attach firmly to a work surface. The optical square mount was designed to alleviate these problems.

Since a major use of the laser measurement system is to calibrate machine tools, it is important that the fixtures and mounts be compatible with standard machine requirements. For this reason, a knee block or right-angle plate

Mechanical Design Features
of the Laser Head

by Charles R. Steinmetz

The product definition for the new 5528A Laser Measurement System placed particular emphasis on low manufacturing cost and ease of use. The laser head (see Fig. 1) is a major component of the system, and requires many complicated mechanical parts. Emphasis was put on low part costs for as many of these mechanical components as possible. Fabrication processes were selected with this in mind.

An important design goal was that these instruments be easy to repair in the field. The main subassemblies are designed to be easily replaceable in the field without disturbing any fixed alignments.

Low-Part-Cost Design

To meet the low-cost goal, designs were made and fabrication processes chosen so that as few parts as possible require a second fabrication process. Some of the processes are die casting, plastic molding, and screw machining.

The two largest components used in the laser head are the laser base and the tube housing. Both are aluminum alloy die castings. These parts make up the structured body of the instrument, so they had to be rigid enough to hold the alignment geometry of all the optical components within the laser head.

Since these parts are die cast, features are easily incorporated, such as cooling fins on the laser tube housing, locating tapers, kinematic mounting legs, printed circuit board mounting bosses, and shielding. Where subsequent machining is required for tapered holes and tighter-tolerance hole locations, extra material is added.

The laser head also contains four plastic molded parts. Two are used in the beam sampler assembly and two in the turret assembly. The beam sampler requires precise angles for mounting the optics contained in the assembly. It has to be compact to minimize beam deviations and sealed to keep out stray light. The plastic parts are molded of ABS plastic and incorporate features such as precise angled mounting surfaces for locating two beam splitters, and slots for positioning a polarizer and a liquid-crystal shutter. The two parts snap together to make a light-tight assembly that has a molded-in locating feature for positioning in the laser base.

The turret assembly, which is visible at the front end of the instrument, contains four sheet-metal parts and two plastic molded parts. The two plastic parts are molded of Delrin™, an acetal resin, which has low friction and good wear resistance. Both parts require these properties. The two parts are the turret base that holds the rotatable shutters in position and the straightness mount that rotates with respect to the fixed turret base and the laser base. These parts also have molded-in features for locating indexing balls for the shutters on the turret base, a recess for the sheet-metal turret face to snap into, mounting surfaces for optics on the straightness mount, and a cantilever spring finger for indexing the part when rotated.

The new straightness optics are part of the 5518A Laser Head. On the older 5500C Laser Head, an add-on optics assembly had to be attached to the front end of the head for making straightness
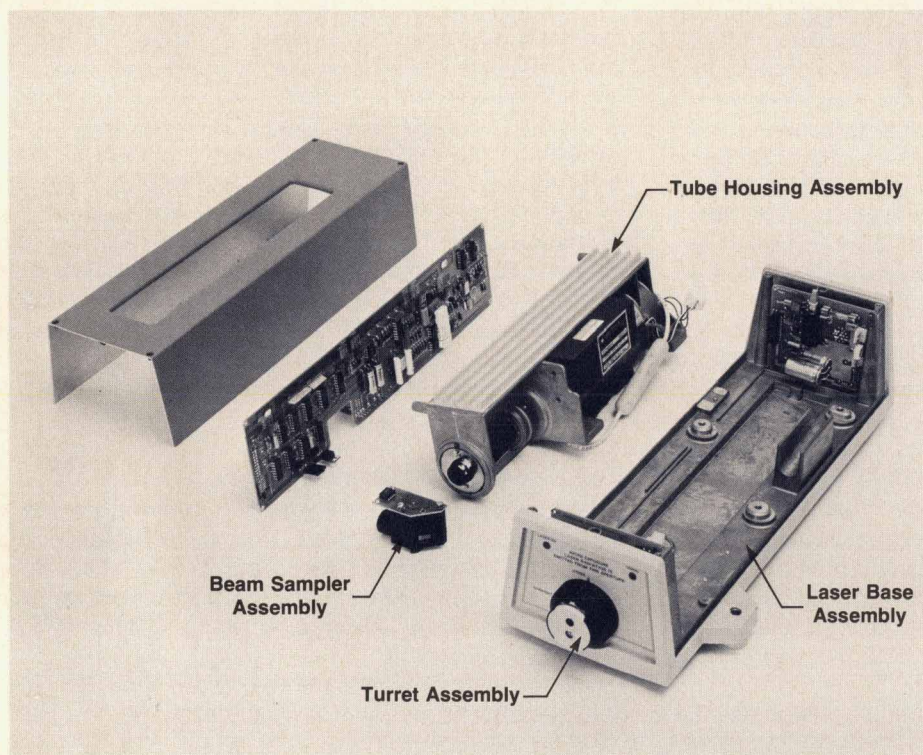

Fig. 1. *5518A Laser Head.*

measurements.

Modular Design

The major assembles in the laser head are designed to be field-replaceable modules with no adjustments required. This means that the alignment between the laser tube housing, beam sampler and turret assembles is critical and must be as free as possible of tolerance buildup. Each assembly has critically aligned components that must be as free as possible of assembly errors. Alignment between these assemblies is held by locating them on the laser base, which has machined mounting surfaces for them.

The printed circuit boards are positioned in the laser head with features that are part of the laser head casting, and are fastened with screws. The boards are interconnected with edge connectors.

The laser tube housing assembly incorporates a positioned laser tube, a collimating telescope, and a waveplate assembly. These components are adjusted to each other to give the required laser beam characteristics. The tube housing assembly is kinematically mounted onto the laser base and is fastened to it with three screws that are accessible from the top of the instrument. This prealignment and accessibility are convenient for built-in applications, where the alignment of the system must not be disturbed when a tube housing assembly is replaced.

The beam sampler assembly also has interconnecting features on both parts. This assembly is fastened to the laser base by two screws and is easily accessible from the top of the instrument.

The straightness mount assembly contains two prealigned beam splitters and is captured between the turret base and the laser base casting. It is located at the front end of the instrument and is accessible by removing the two screws that fasten the turret base to the laser base.

Charles R. Steinmetz
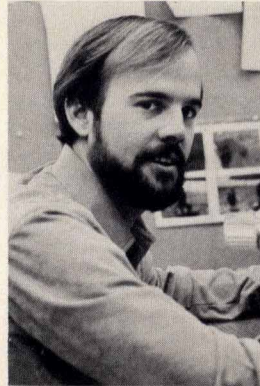
Charlie Steinmetz was responsible for the product design of the optical components and parts of the laser head for the 5528A Laser Measurement System. With HP since 1978, he's also designed vacuum and high-pressure systems used in frequency standard production. He was born in Palo Alto, California and received his BSME and MSME degrees from the University of California at Berkeley in 1976 and 1978. A scuba diver and underwater photographer, he enjoys vacationing where the ocean is clear and warm. He and his wife live in Cupertino, California and are expecting their first child.

concept is used. The 10777A Mount is a fairly massive investment-cast stainless-steel design. It has cast-in clamp pads that clearly identify areas for securing it to a machine bed. These are all located opposite ground contact pads to eliminate the possibility of distortion caused by heavy clamp pressure applied in the wrong areas. Except for the contact pads, the entire casting is texture-finished for a good appearance.

The optical square is easily attached to the mount and removed from it by means of a single threaded post built into the mount. The widely spaced contact pads ensure repeatability of location. The 105-mm centerline is achieved in both horizontal and vertical positions.

The contact pads are precision-ground to be parallel and perpendicular to the optical square pads. The design of the optical square makes it insensitive to rotation (within the window aperture range) normal to the beam reflected plane. For this reason the mount is designed to maintain accuracy in only two axes.

Used in the vertical position, the assembly can be used for vertical straightness measurements. The 10772A Turning Mirror and its leveling mount can be attached directly to the optical square. This combination in turn is attached by the 10777A Mount to the machine bed. All location requirements for these optics are automatically met, eliminating much of the setup drudgery. Since the entire assembly is clamped to the machine bed, measurements can be performed without fear of accidentally bumping and moving the components or of machine vibration altering the measurements.

Flatness Mirror

The 10773A Flatness Mirror is used in conjunction with the angular optics system to calibrate surface plate flatness. It consists of a mirror mounted vertically in a frame that can rotate 360° on a rectangular base plate. The mirror remains in a precise vertical plane at all times with respect to the surface plate.

A major design feature of this mirror is that with its extended base, virtually the entire area of a surface plate can be characterized. By positioning the base of the mirror on the edge of the surface plate and allowing that portion containing the mirror to hang over, the angular optics can be positioned to measure surface flatness within an inch of the edges. Previous designs would not allow measurement of a peripheral band approximately three inches wide along the edges of the surface plate.

The 55282A Flatness Accessory Kit contains two flatness mirrors and the 10759A Footspacing Kit. With two mirrors, a full surface plate characterization can be accomplished with one setup of the laser head. The angular interferometer is attached to the flatness mirror base and the angular reflector is attached to one of the three precision-ground footspacing kit bases, depending upon which surface contour interval is being inspected. By moving the reflector/footspacing assembly along a straightedge on the surface plate, and recording angular data at fixed intervals, a full surface plate contour plot can be made.

Tripod-to-Laser-Head Adapter Plate

The 10753A Tripod provides an adjustable mount for the 5518A Laser Head. The lower portion of the tripod is fundamentally the same as the 10580A Tripod for the earlier 5526A Laser Measurement System. The adapter plate for the new 5518A Laser Head, however, has been completely redesigned.

The major design improvements the user will see are the fine adjustment mechanisms for aiming the laser beam. These allow for precise directing of the beam in pitch and yaw. The adjustment controls are conveniently located at

the rear of the 5518A Laser Head. The laser is attached to the tripod with two large socket-head screws. This is a very quick operation. It provides a positive and secure connection along with flexibility for the beam alignment setup process.

Pitch of the laser beam is controlled by turning a threaded shaft that runs through the rear footpad of the laser head. It provides an adjustment range of $\pm 3°$ in the pitch angle of the 5518A relative to the tripod. After the proper angle has been established during the setup procedure, it can be secured by a built-in jam nut which locks the adjustment screw. All of these controls are hand operated and require no special tools.

The yaw adjustment is built into the rear portion of the tripod adapter plate. The laser head can be rotated $\pm 4°$ with respect to the tripod base. The adjustment mechanism consists of a fine-threaded cross slide and shaft. A large hand knob provides a convenient crank and a thumbwheel for greater control.

A multiaxis pivot mechanism is located near the front of the adapter plate. It attaches the pivot arm of the tripod adapter plate to the baseplate. Flexibility in both pitch and yaw of the 5518A is provided while firmly securing it to the tripod. Both movements can be locked by a hand knob located just under the pivot bolt. It has a built-in spring load that ensures firm contact between components at all times. Most users will find that this spring load is sufficient to provide a stable position for the laser head during measurements, but the hand knob can be tightened if desired. To ensure smooth movement between the laser head and baseplate, the pivot arm contains two brass inserts that are cylindrically shaped to coincide with the pivot pitch radius. The base contains two corresponding hardened and polished steel inserts. Even with the pivot bolt drawn down fairly tight, the sliding action remains smooth.

A bubble level is built into the base. This allows for initial leveling of the tripod leg assembly on virtually any surface. The tripod has a durable black textured finish.

Computer Modeling

The optical system of the 5528A Laser Measurement System was modeled so that a computer could be used to develop specifications for measurement ranges and optical separation distances. Modeling provided the tool to determine the appropriate combinations of lower-level specifications needed to provide maximum performance of the system. The measurement versatility of the 5528A System introduces a large number of optical cases, which can best be handled by a comprehensive computer modeling technique.

The optical system model combines several nonlinear functions of many variables. These functions were determined by both empirical and theoretical methods.

The laser beam consists of two coaxial beams of slightly different frequencies, and it is the difference frequency (plus Doppler shift) that generates the measurement signal. Since the two beams must interfere to produce a signal, they must overlap coaxially by a significant amount to generate an acceptable signal. The two beams take different paths in a measurement and are subject to changes in angle, wavefront distortion, axial alignment, and diameter. As these

changes increase, the two beams overlap less and generate less signal. Once a minimum signal level is chosen, integration over the beam overlap region on the receiver determines the necessary signal power. Since the functions are nonlinear, a high-accuracy numerical integration technique is used.

The intensity profile of the beams is Gaussian, and the width of the profile is a function of the optical path traveled. The intensities of the two beams, $I_{reference}$ and $I_{measure}$, can be written in polar coordinates as:

$$I(r,w) = I_o\, e^{-2r^2/w^2}$$

where r is the radial component and w is the spot size of the beam. The spot size w is the 2σ point of the Gaussian profile. It increases because of diffraction spreading and collimation of the beam. This increases the diameter of the beam and changes the power density. Signal power loss is heavily dependent on this beam spreading. The other major power loss is from beam alignment. The beams must interfere on the detector, and because their profiles are Gaussian, small movements off the receiver result in large power losses. Air turbulence and temperature gradients are also first-order factors, but they can be controlled and stabilized so that their effects are virtually eliminated.

Secondary power losses come primarily from phase losses between the two interfering beams. These losses occur from wavefront distortion caused by the optics, radius of curvature changes between the two beams, and small axial angles between the beams. Lower-order losses include incoherence, absorption, scattering, and optics efficiencies. Integration of the product of these functions produces the overall signal power. The overall power can be normalized to an ideal case to give a relative signal power for the particular optical case. Integration limits are defined by the effective receiver radius. Relative signal power is generated by the evaluation of:

$$\begin{aligned}
\frac{\text{Receiver}}{\text{Power}} &= E \times V(\Theta_1,\Theta_2) \times S(z,A) \times L(z) \\
&\times \iint\limits_{\substack{\text{detector} \\ \text{area}}} \Big[\, \big[I_{ref}[r,z,D(z,\Omega_1,\Omega_2),\, P(T),\, W(z,K(z,t)),\, G(t)] \big] \\
&\times \big[I_{meas}[r,z,D(z,\Omega_1,\Omega_2),\, P(T),\, W(z,K(z,t)),\, G(t)] \big]^{1/2} \\
&\times R(r) \times C(z) \times dA
\end{aligned}$$

In this equation,

z = optical path length of beams (OPL)

r = radial component (beam offset)

$D(z,\Omega_1,\Omega_2)$ = beam offset on detector caused by optics wedges and OPL

$W(z,K(z,t))$ = spot size as a function of OPL and collimation, where collimation is a function of OPL and temperature

$R(r)$ = photodetector response over surface

$C(z)$ = phase loss caused by radius of curvature differences

$G(t)$ = initial Gaussian beam alignment (temperature dependent)

$P(T)$ = pointing stability as a function of time

E = optics transmission efficiencies

$S(z,A)$ = scattering and absorption as a function of OPL and air quality

$V(\Theta_1, \Theta_2)$ = loss from nonparallelism of wavefronts and optics figures

$L(z)$ = coherence loss

The model prompts the user for fixed variables, and then generates the signal power as a function of optical path length (range).

Results from the model are in very close agreement with data accumulated from experimental testing. Several versions of the model allow the performance of each 5528A measurement mode to be predicted accurately.

Acknowledgments

A number of production engineers and manufacturing personnel have contributed significantly to the success of the 5528A Laser Measurement System. Among these are Jeff Benzing who worked on the design of the laser tube process station. John Tsai was responsible for the optics coating analysis and testing. Fred Turner and Merv Hopson did the production engineering development work on the fabrication and assembly of the optics and laser tube. Glenn Burgwald was instrumental in the early engineering design efforts on the tube. Dave Gottwals' manufacturing engineering group has been working closely with the design team from an early date. The design of much of the automated tooling to process and assemble fabricated parts can be credited to their efforts. Ernie Riberdy was responsible for designing and building the highly specialized machine that fabricates the laser rod. Ernie was also involved in a number of other process and tooling efforts on the project. Paul Conrotto had major responsibility for the manufacturability of all the optical housings. Doug Thomas had a key role in getting the laser head die castings and sheet metal components through their machined process operations. Dave Gottwals was involved in the very early design phases of the 5518A die castings. He was also responsible for the manufacturing and tooling for the tripod adapter. Jerry Curran did much of the manufacturing work on the sheet-metal parts in the project. Much of the manufacturing work on the plastic components in the project was done by Ashok Phadke. A large thanks is extended to Bob McKee and Harry Thomas's model shop group for their contribution in supplying prompt turnaround and quality of prototype parts. Ken Wayne joined the project to accept responsibility for the entire laser tube. His efforts required him to work closely with manufacturing to fabricate and assemble the critical components of the tube. Roger Leavitt, one of the early project team members, originally had responsibility for a broad range of product design tasks including die casting, plastic molded parts, and laser tube parts. As the project team grew he concentrated on the laser head castings and sheet-metal designs along with the system cables and several major plastic components. Chuck Lowe joined the project team in early 1982. He completed the design of the new tripod adapter plate and the optics carrying cases. A special thanks goes to Pam Blizzard, our financial accountant, who has monitored the project costs and time standards through the many design phases.

References

1. R.R. Baldwin, G.B. Gordon, and A.F. Rudé, "Remote Laser Interferometery," Hewlett-Packard Journal, Vol. 23, no. 4, December 1971.
2. R.R. Baldwin, B.E. Grote, and D.H. Harland, "An Interferometer That Measures Straightness of Travel," Hewlett-Packard Journal, Vol. 25, no. 5, January 1974.

Larry E. Truhe
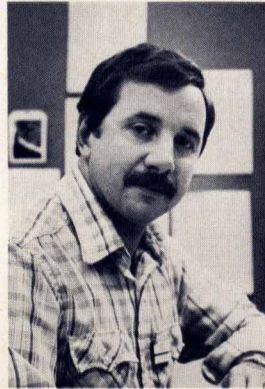
Larry Truhe is project manager for the 5528A Laser Measurement System optical components. He received his BSME degree in 1967 from South Dakota School of Mines and Technology, then spent six years as a manufacturing engineer before joining HP in 1973. Before becoming an R&D project manager, he served as a production engineer and manufacturing engineering manager for HP's Stanford Park Division. Larry is married, has three children, and lives in San Jose, California. Although they enjoy traveling and camping, Larry's family is heavily involved in soccer. He has served as coach, referee, and club officer for various youth soccer programs.

Richard R. Baldwin
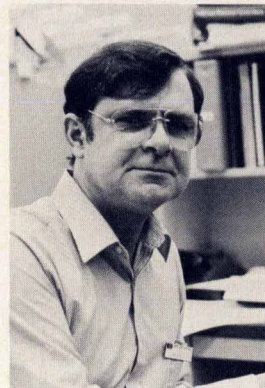
Dick Baldwin has been developing laser interferometer products for HP since 1969, except for one three-year term as a manufacturing engineer. A former U.S. Navy officer and metrologist, his work has resulted in five patents on interferometers and optics and seven papers, including three HP Journal articles, on interferometers and machine tool calibration. A member of the Optical Society of America, he received his BS degree in engineering physics from Ohio State University in 1959. He is married, has two children, lives in Saratoga, California, and enjoys sailing. He's a native of Springfield, Ohio.

David C. Woodruff

Dave Woodruff received his BS degree in physics from the University of Southern California in 1981, then joined HP's Santa Clara Division. He's been responsible for developing photometric techniques for testing the optics of the 5528A Laser Measurement System, for computer modeling of the optics, and for supporting the optical coating operation. Born in Fullerton, California, he's married, has a son, and lives in Los Gatos, California.

Noise Figure Meter Sets Records for Accuracy, Repeatability, and Convenience

Noise figure measurements used to be mysterious, time consuming, difficult, and not very accurate. This instrument makes them quick, accurate, and easy.

by Howard L. Swain and Rick M. Cox

I T HAS BEEN TWENTY-FOUR YEARS since Hewlett-Packard introduced its first noise figure meter,[1,2] and noise figure is still a widely used figure of merit for the noise performance of devices, subassemblies, and complete systems.* As performance requirements have increased, it has become increasingly important to be able to measure noise figure accurately and conveniently. For example, a 0.34-dB difference in the noise figure of low-noise amplifiers for satellite earth stations can translate into a fivefold difference in price.[3]

The new HP Model 8970A Noise Figure Meter (Fig. 1) makes outstanding contributions to this field in accuracy, convenience, and flexibility. The use of a microprocessor enables it to correct several of the errors that have been accepted as part of the measurement uncertainty in the past. Its own broad tuning range, high sensitivity, and ability to control external local oscillators over the HP-IB (IEEE 488) provide a tremendous increase in convenience. The 8970A can also measure gain and display both swept noise figure and gain as functions of frequency on an oscilloscope. Thus it can gather data in a few minutes that would take hours by previous methods. It turns a mysterious, time consuming, difficult, often inaccurate measurement into one that is quick, accurate, easy, and pleasant.

*Some basic noise figure theory is presented in the Appendix at the end of this article.
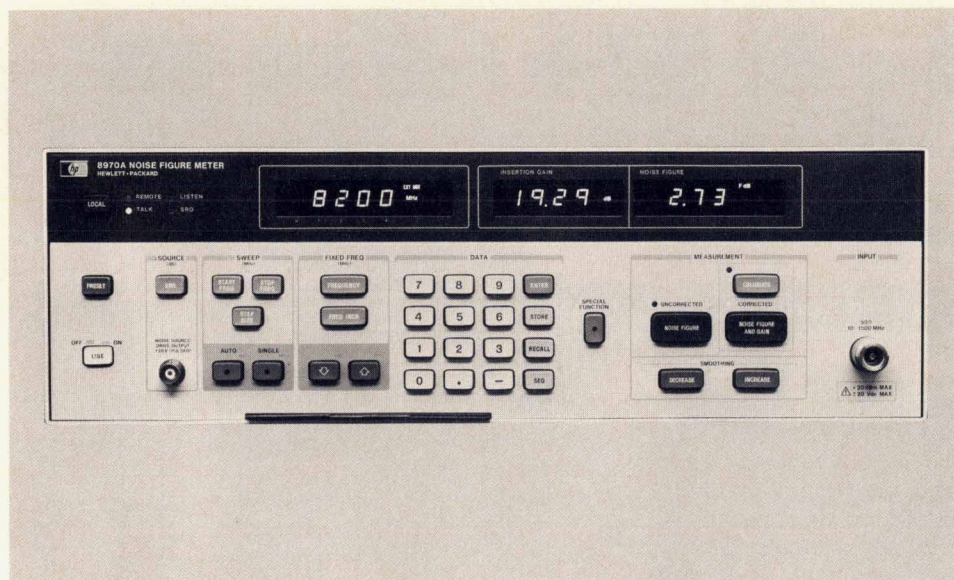
8970A Contributions

Three effects that have caused errors in noise figure measurements in the past are eliminated by the 8970A. The first is the variation with frequency of the excess noise ratio (ENR) of the noise source used for the measurements.* The ENR of the source must be known before the noise figure of the device under test can be measured. While some noise figure meters allow the entry of an arbitrary ENR, only one value can be entered. When a measurement is taken at a new frequency, a new value has to be entered. Thus measurements must be made at one frequency at a time.

The 8970A allows the entry of ENR for 27 frequencies at one time and stores this data in a table. When a measurement is made, the proper value is automatically used for that frequency. If necessary, the 8970A interpolates linearly between the entered data points.

The second error arises because the off or cold noise temperature of the noise source, T_C, is not equal to the standard reference temperature of 290K. T_C is equal to the physical temperature of the noise source termination, which is approximately room temperature or about 296K. This 6K error in T_C causes an error in noise figure of about 0.1 dB for noise figures below 1 dB. Assuming that $T_C = 290K$, as all previous noise figure meters do, simplifies the equation* enough that it can be solved by analog circuits. How-

*See Appendix.

Fig. 1. *Model 8970A Noise Figure Meter measures noise figure, effective input noise temperature, and gain, contributing less than ±0.1 dB of uncertainty to noise figure measurements. A built-in microprocessor corrects automatically for ENR variations and second-stage effects.*

ever, the 8970A's microprocessor easily solves the exact equation, virtually eliminating this error.

The third error is caused by the second-stage noise figure. When the noise figure of two devices in cascade is measured, the result F_{12} includes contributions from both devices: $F_{12} = F_1 + (F_2 - 1)/G_{av1}$, where F_1 is the noise figure (in ratio form) of the device under test, F_2 is the noise figure of the second stage, and G_{av1} is the available power gain of the first stage. In a calibration step, the 8970A measures and stores its own noise figure F_2. Then when it measures the gain of the device and the total noise figure F_{12}, it can solve the above equation for the noise figure of the device alone, F_1. Since the gain and noise figure are measured at the same time, the 8970A can display the corrected noise figure in real time. This is extremely important, for example, when tuning a transistor to find the minimum noise figure. Because the tuning also affects the gain, it is essential to make this correction in real time to find the true minimum of F_1. If F_{12} is minimized and then that minimum is corrected for second-stage noise, the result is a different, higher, and wrong number because the tuning is a compromise between what minimizes F_1 and what maximizes G_{av1}. Before the 8970A it was almost impossible to make this measurement to find the true minimum of F_1.

Two additional factors can reduce the accuracy of the measured noise figure. The first is a lack of adequate resolution. The 8970A has 0.01-dB resolution to go with its 0.1-dB accuracy. To avoid any possibility of roundoff or other errors, the data sent out on the HP-IB has 0.001-dB resolution.

The second factor is lack of adequate smoothing or filtering to make use of the high resolution. The 8970A uses adjustable exponential averaging during fixed-frequency measurements.[4] Two front-panel keys, **INCREASE** and **DECREASE**, allow the user to adjust the smoothing for an optimum tradeoff between speed of response and jitter. Even when increased averaging is selected, the 8970A still updates the display three to five times per second, making adjustments easy. During sweeps, the 8970A averages the selected number of readings at each frequency before moving on.

Besides the errors described here, many inconveniences have plagued those who attempt to measure noise figure. First, all previous noise figure meters measure at only one or a few fixed frequencies. Measurements over a band of frequencies require an additional mixer and a tunable low-noise local oscillator. Some noise figure meters require the use of an additional amplifier. It is almost impossible to make swept, single-frequency measurements over a broad bandwidth. The 8970A remedies all of these shortcomings. It tunes from 10 to 1500 MHz in 1-MHz (or greater) steps, and it has enough internal gain so that no additional amplifiers are needed. Thus, the 8970A and a noise source can measure a great many devices without any additional equipment.

To measure noise figure at frequencies above 1500 MHz does require an external mixer and local oscillator. However, even this measurement is easy. All parameters (ENR, T_C, and frequencies) are still entered into the 8970A, and the 8970A acts as a limited HP-IB controller to set the frequency of the external local oscillator. Naturally, all the corrections mentioned above are still made. For example, using the HP 8672A as an external local oscillator allows the user to make a swept, fully corrected noise figure and gain measurement from 2 to 18 GHz and have a flicker-free display on a nonstorage oscilloscope.

Because the 8970A can correct for second-stage noise figure, it can measure the noise figure of lossy devices such as mixers. With its broad frequency range, the 8970A can even measure noise figure as a function of intermediate frequency (IF).

For low-noise devices and for use in systems calculations, many users want their measurement results in terms of effective input noise temperature T_e instead of noise figure. The 8970A can accommodate them. In addition to noise figure in dB and T_e, the 8970A can also display noise figure as a ratio and Y factor (see below) as a ratio and in dB.
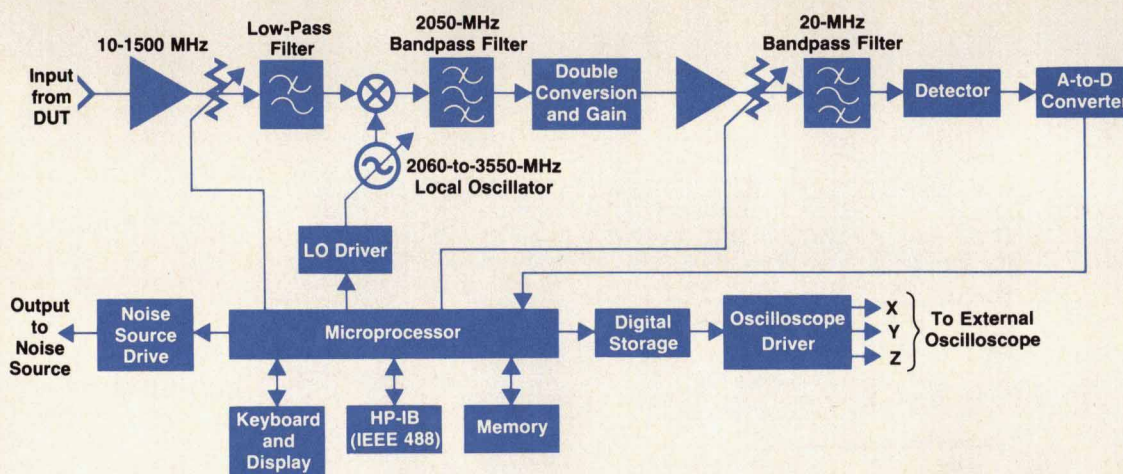
Fig. 2. The 8970A Noise Figure Meter is basically a tunable power meter or receiver. The microprocessor controls the input and IF attenuators and the first LO, reads the analog-to-digital converter, provides output data to the digital storage circuits, and turns the noise source on and off.

System Design

There are many ways to measure noise figure.[5] All techniques require at least two measurements of the output power from the device under test (DUT). For the first measurement, the signal connected to the input of the DUT is noise of a known power P_1. For the second, the signal is noise or a single-frequency continuous-wave (CW) signal of a different known power P_2.

The first thing to decide is whether to use noise or CW for P_2. The use of CW has several disadvantages: it requires that the bandwidth of the measurement be accurately known, it is difficult to know the absolute power of low-level CW signals, and a broadband (10 MHz to 18 GHz) CW source is rather expensive.

On the other hand, the advent of solid-state noise sources has provided a broadband, inexpensive source for P_2 that can be accurately calibrated in power level. Furthermore, the use of noise eliminates the need to know the measurement bandwidth accurately. Therefore, noise was chosen for P_2 in the 8970A.

The 8970A needs to measure the ratio of P_2 to P_1, known as the Y factor. There are many ways to do this, depending on whether P_2 is varied and whether Y is forced to be 2 (the 3-dB method) or not.[5] The most accurate way that is also convenient is to keep P_2 fixed, let Y vary as determined by the DUT, and measure the ratio of P_2 to P_1 with a power meter. This is the technique automated with the 8970A.

Although the quantity of interest is spot noise figure,[6] that is, noise figure at one particular frequency, in practice one can only measure noise averaged over a band of frequencies, the measurement bandwidth. Therefore, a noise figure meter must define the measurement bandwidth and select the center frequency of that bandwidth. Hence the 8970A is really a tunable power meter or receiver (see Fig. 2).

It is easiest and most accurate to do most of the signal processing at some intermediate frequency. Therefore, some frequency conversion is needed to translate the input frequency to that IF. To measure noise figure at only one frequency, the noise figure meter must reject the image and other responses of the input mixer.

There are two ways to do this. One is to use a preselector. The other is to have the first mixer up-convert the input signal to a first IF that is higher than any desired input frequency. This has two advantages over preselection. First, a simple fixed low-pass filter rather than a tunable low-pass or bandpass filter can be used. This is important when a range greater than two decades must be covered. Second, the first local oscillator (LO) has to tune less than an octave to provide greater than two decades of frequency coverage. Therefore, the 8970A uses the up-convert method.

As can be seen in Fig. 3, the 8970A down-converts from the first IF of 2050 MHz to the last IF of 20 MHz in two steps. This helps eliminate undesired responses. An isolator be-
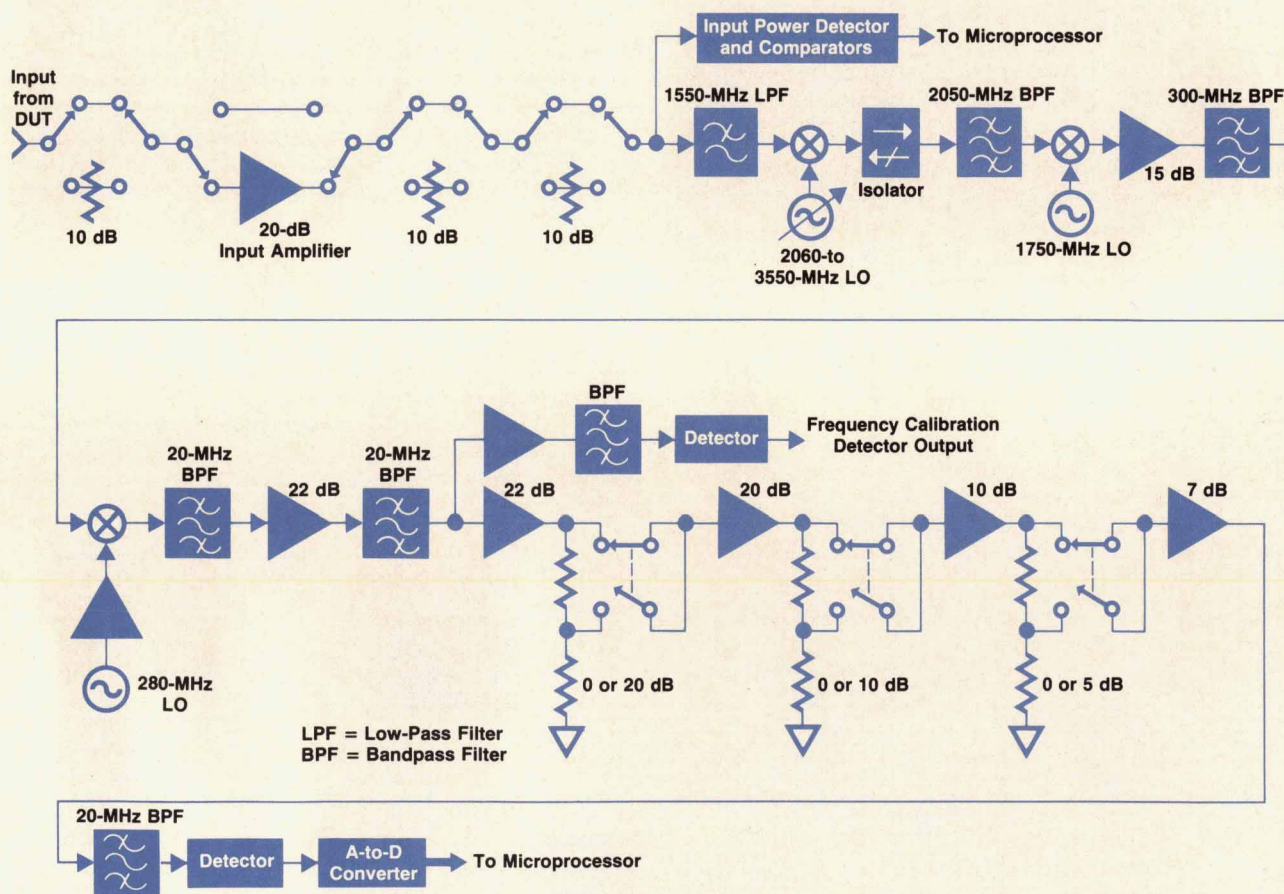

Fig. 3. 8970A RF block diagram. Input signals are converted to a 20-MHz IF for processing. Gain, filtering, and step attenuation are distributed along the IF chain.

A Noise Source for Noise Figure Measurements

The noise source used for a noise figure measurement is the standard of the measurement, that is, the calibration and accuracy of the noise source are transferred directly to the measurement. For the noise characteristics of devices to be easily verifiable at vendors' and customers' plants, noise sources must be stable and accurately calibrated.

The source impedance of an ideal noise source is exactly equal to the characteristic impedance of the system in which the device under test is intended to operate—50 ohms is the most common value. Because the measured noise figure of many devices is a sensitive function of the source impedance, any deviation of the noise source impedance from the nominal value introduces errors into the measurement. These errors require correction if accurate comparisons are to be made using different measurement systems. Therefore, for rapid, convenient, easily comparable measurements, the noise source should have an impedance as close to 50Ω as possible. The source should also be useful over a wide frequency range.

These requirements governed the design of the 346B Noise Source and had considerable impact on the specifics of its implementation. The noise generator in the 346B is a specially constructed silicon diode operated in avalanche breakdown to achieve the hot temperature or on condition.[1,2] To ensure that the diode breakdown characteristics and the resulting noise spectrum are consistent from diode to diode and each time each diode is turned on, the anode is surrounded with a guard ring, as depicted in Fig. 1. The guard ring region has a higher breakdown voltage than the anode and confines the breakdown region to the area directly under the anode, thereby eliminating edge effects that can cause fluctuations in the noise spectrum. The active area of the diode is small to minimize the effects of material inhomogeneities.

The diode chip is mounted directly on the metal cartridge for optimum heat sinking to maintain the lowest possible junction temperature and best long-term stability of the calibration.[3,4]

It was desired that the 346B Noise Source have wide bandwidth, both for measurement convenience and for the economy resulting from needing only one source for a broad range of applications. However, the diode impedance varies greatly over the desired frequency range of 10 MHz to 18 GHz, so it was essential to develop an imbedding circuit that matches the diode impedance to 50 ohms and simultaneously provides a flat ENR-versus-frequency characteristic. This is done by using a combination of loss and reactive matching as indicated in the equivalent circuit shown in Fig. 2.

As shown in Fig. 3, the noise diode and matching circuit are sealed in a hermetic package. A wideband hermetic feedthrough
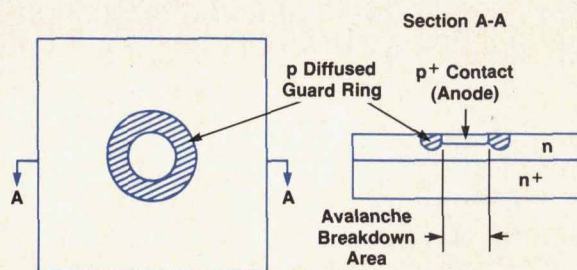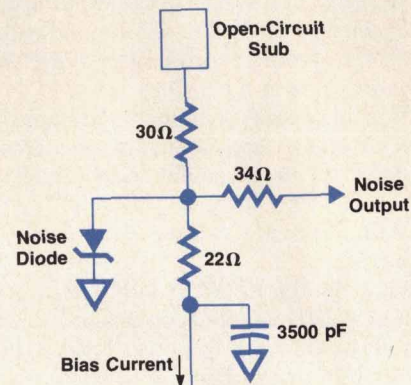
Fig. 2. Schematic diagram of the broadband impedance-matching imbedding circuit for the 0.01-to-18-GHz noise diode.

was specially developed to provide a low-SWR transmission structure and to form part of the mechanical transition from the 3.5-mm coaxial structure external to the noise cartridge to the microstrip matching circuit within the cartridge. An internal transition from 3.5 mm to 7 mm is used when type N or APC-7 connectors are desired. To improve the source match, a 6-dB pad is used between the external connector and the noise cartridge, providing an additional 12-dB improvement in the return loss. Fig. 4 shows the typical source match of the 346B Noise Source.

The available noise power produced by the avalanche process is inversely proportional to the diode current. Therefore, it is important that the current be well controlled to obtain repeatable results. The 346B contains a built-in current regulator to ensure the correct value of diode current under all conditions, such as might occur with different drive cable lengths or operation from a supply separate from the 8970A. The diode current for each 346B is factory adjusted to the optimum value during the calibration procedure.

ENR Calibration

Because solid-state noise sources are not fundamental standards, they must be calibrated using a fundamental standard, namely a physically heated or cooled resistor. The United States National Bureau of Standards (NBS) provides regular calibration service only at the frequencies shown in Fig. 5, using resistive terminations that are at the temperatures listed.
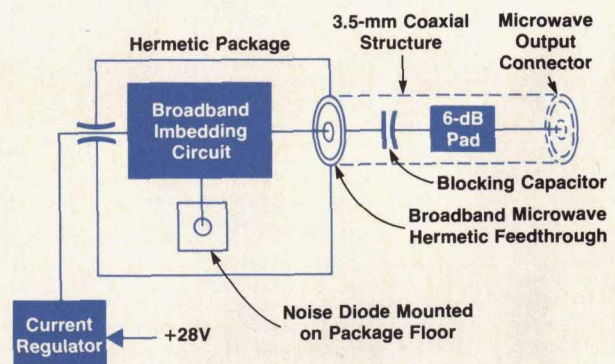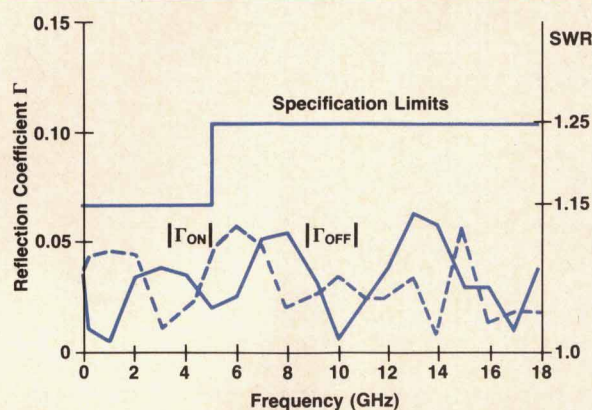
Fig. 1. Noise diode guard ring detail. The guard ring ensures consistent avalanche breakdown characteristics.

Fig. 3. Block diagram of the HP 346B Noise Source.

Fig. 4. *Typical source match of the 346B Noise Source.*

Fig. 5. *Traceability of 346B Noise Source calibration to the United States National Bureau of Standards.*

The standards laboratory of Hewlett-Packard's Stanford Park Division regularly sends its transfer standard noise sources to NBS for calibration. For the frequencies at which NBS does not provide service, the SPD standards lab maintains hot and cold loads for use as standards. Cross checks are done between the transfer standards and the hot and cold loads and between the two waveguide transfer standards to assure the highest possible confidence.

Then the transfer standards and the hot and cold loads are used to calibrate four solid-state noise sources (346Bs) to be used as working standards in production. These working standards (one for each connector option) are used to calibrate the units for shipment.

References

1. R.H. Haitz, "Noise in Self-Sustaining Avalanche Discharge in Silicon: Low-Frequency Noise Studies," Journal of Applied Physics, Vo. 38, no. 7, June 1967, pp. 2935-2946.

2. R.H. Haitz and F.W. Voltmer, "Noise in a Self-Sustaining Avalanche Discharge in Silicon: Studies at Microwave Frequencies," Journal of Applied Physics, Vol. 39, No. 7, June 1968, pp. 3379-3384.
3. M. Kanda, "An Improved Solid-State Noise Source," IEEE Transactions on Microwave Theory and Techniques, Vol. MTT-24, no. 12, December 1976, pp. 990-995.
4. M. Kanda, "A Statistical Measure for the Stability of Solid-State Noise Sources," IEEE Transactions on Microwave Theory and Techniques, Vol. MTT-25, no. 8, August 1977, pp. 676-682.

-Donald R. Chambers

tween the first mixer and first IF filter minimizes reflections and assures a smooth frequency response. The losses of the first two mixers, the isolator, and the 1550-MHz and 2050-MHz filters, combined with the noise figure of the 15-dB, 300-MHz amplifier result in a 15-dB noise figure looking into the first mixer.

Adding a low-noise 20-dB amplifier to the input reduces this noise figure to about 6 dB at low frequencies. High input powers from high-gain devices under test make it necessary to switch out the input amplifier and add some attenuation. The microprocessor reads a detector at the input to the first mixer to keep the level incident on the mixer below −20 dBm when the noise source is turned on.

Filtering is distributed in the 20-MHz IF. The first filters keep the 280-MHz LO feedthrough and the total broadband noise from overloading the amplifier stages. The last filter makes sure the detector responds to the noise in only the 4-MHz bandwidth. The step attenuators are also distributed so the noise figure can be kept low and the amplifiers are not overdriven. These IF step attenuators and the input RF step attenuators are kept fixed as the noise source is turned on and off for P_2 and P_1. Thus their attenuation errors do not affect the Y-factor accuracy.

There are several tradeoffs in selecting the IF bandwidth and the integration time of the analog-to-digital converter (ADC) that measures the detected power level. Whenever noise power is detected (converted to dc), the resulting dc is noisy. For the 8970A's detector the noise-to-signal ratio is $1/\sqrt{B\tau}$, where B is the predetection (IF) noise bandwidth and τ is the postdetection filter time constant. Thus, for minimum display jitter, both B and τ should be maximized. A large B also minimizes susceptibility to electromagnetic interference (EMI). Because the "signal" is noise, a larger B makes a larger "signal."

An ADC that integrates the input signal can provide the needed postdetection filtering. This is advantageous because the microprocessor can turn the integrator on and off in synchronism with the noise source drive. Thus, the 8970A does not have to wait many time constants for a separate filter to reach steady state before the A-to-D conversion can take place. Filtering and conversion happen at the same time with one circuit doing both. In this case, the filter time constant τ is just the integration time. Therefore, a large τ also makes it easier to build an ADC with the ≥14 bits required to make its quantization error less than 0.005 dB.

On the other hand, if B is too large, the measurement is no longer of spot noise figure, especially at the lowest RF measurement frequency of 10 MHz. Furthermore, it becomes harder to measure narrowband units. If τ is too large, the reading update rate will be too low, making it hard to adjust or tune a circuit for minimum noise figure.

Verifying the 8970A's Accuracy in Production

The signal path of the 8970A Noise Figure Meter can be described as a receiver that has up to 100 dB of very stable gain, followed by a noise power detector and an analog-to-digital converter. To verify that the 8970A meets its noise figure accuracy specifications, the linearity of these circuits must be measured during production testing.

To measure the 8970A's amplifier, detector, and analog-to-digital converter linearity over a 22-dB range with 0.001-dB resolution, the automatic test system shown in Fig. 1 is used. Typical repeatability of this system is about 0.005 dB.

The test system measures the 8970A's linearity by comparing the output of the 8970A's detector to that of an 8484A Power Sensor and a 436A Power Meter as their common input power level is stepped over the 22-dB range. Using a power meter to measure the input power to the 8970A at each step eliminates errors caused by test system input attenuator inaccuracies, non-repeatability, and mismatch.

Errors caused by nonlinearity in the power sensor are greatly reduced by operating the sensor over only a 5-dB range, from −38 dBm to −43 dBm. Over this range, the sensor and power meter are linear within 0.005 dB and measurement noise and drift are negligible. Reading the power meter's recorder output with the 3456A Digital Voltmeter gives greater resolution than is available from the power meter's HP-IB output. The entire reference channel is periodically calibrated by the HP standards laboratory.

After the correct starting power levels are set up, readings are taken from each channel. Then the test system input attenuation is increased and the change in power in both channels is measured. This change in noise power should be equal for both the reference and test channels. Any difference between the two is the linearity error of the 8970A under test (see Fig. 9 on page 31).

This is repeated until the test system input attenuation has been increased by 5 dB. Then the reference channel attenuation is decreased by 5 dB, returning the sensor and power meter to the correct operating range for the next measurement. Whenever this attenuator is changed, errors can be introduced by its nonrepeatabilities and mismatch errors and by power splitter tracking errors. To reduce these errors, the test program makes a new reference measurement each time the reference channel attenuator is stepped.

Because noise is used as the "signal," there is noise or jitter in the reference and test channel measurements. This jitter is reduced by using the internal averaging available in the 8970A and the 3456A. Also, a curve fit is done on the final data.

In making a noise figure measurement, the 8970A must make two power measurements—one with the noise source on and one
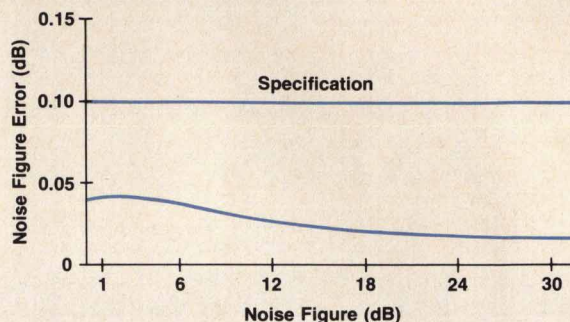

Fig. 2. 8970A noise figure error versus noise figure.

with it off. Their ratio is the Y factor, and its error can be read from the linearity error curve by taking the difference between the errors at the two power levels. For each possible Y factor, the test system program determines Y-factor error for all possible allowed combinations of the two powers from the linearity curve. Then, the worst error is found for each Y factor. Next, the ideal noise figure is calculated for each Y factor. Noise figure is also calculated using these Y factors and the previously calculated worst-case Y-factor errors. The difference between these two noise figures is the 8970A's noise figure measurement error, Fig. 2.

The test system also measures the 20-MHz IF attenuator error, and by combining this with the detector linearity error (Fig. 9, page 31), determines the gain measurement accuracy of the 8970A.

A major benefit of this test system is its flexibility to change. The test noise source can be replaced by a signal generator or broadband noise source. By readjusting the input, reference, and test attenuator levels, power linearity measurements can be made over wide frequency ranges for many devices such as power sensors and microwave detectors.
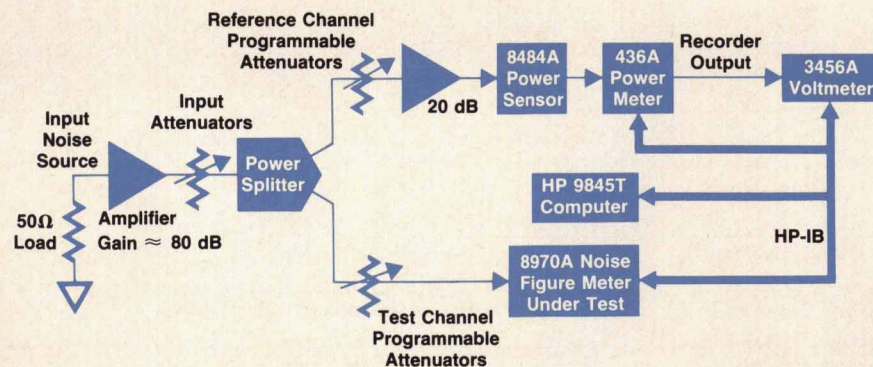
-Harry Bunting

Fig. 1. Test setup for verifying the linearity of the amplifiers, detector, and analog-to-digital converter of the 8970A Noise Figure Meter.

Clearly, a compromise is required. The 8970A has an IF bandwidth B of 4 MHz and an ADC integration time τ of 16 ms. These combine to give a low jitter of 0.05 dB peak, a reasonable spot size, and a reading rate of about five per second, which includes time for two A-to-D conversions and time for the microprocessor to calculate, display, and perform other functions. This compromise made the EMI shielding not too difficult and eased the design of the 16-bit ADC. If less jitter is required, software smoothing can be selected.

Input Assembly

The input assembly (see Fig. 4) serves as a low-noise, broadband, variable-gain front end for the rest of the instrument. It consists of three switchable 10-dB attenuators, a switchable 20-dB low-noise, broadband amplifier, and a power detector. Input noise power incident on the first converter is detected and converted to a dc voltage by the input power detector circuit. This voltage is then sent to a pair of comparators that signal the controller assembly that the input power is either too high, at an acceptable level, or too low. The controller uses this information to adjust the overall gain of the input assembly appropriately. Gain of the assembly is variable in 10-dB steps from -30 dB to $+20$ dB. Optimum power level to the first converter is between -30 dBm and -20 dBm.

A few circuit details of the input amplifier are noteworthy. The amplifier consists of two independent high-frequency-transistor series-shunt feedback stages. This configuration gives an acceptable compromise for overall amplifier noise figure, gain flatness, input match, and

bandwidth for the number of stages used. The input amplifier is realized using printed circuit board technology. This requires parallel combinations of capacitors and resistors in several places to reduce the effects of parasitic lead inductance. The variable inductor in the collector of transistor Q1 is realized by a variable-length high-impedance transmission line. It is used to adjust amplifier gain at high frequencies. Performance specifications for the amplifier are:

Frequency Range	10 to 1500 MHz
Input SWR	<1.5
Gain	20 dB ± 1 dB
Noise Figure	3.5 dB at 10 MHz
	5.0 dB at 1500 MHz
P_{out} at 1 dB compression	>10 dBm

The input power detector consists of a zero-bias Schottky detector diode operating in the square-law region followed by a high-dc-gain operational amplifier stage. Feedback around the op amp includes a thermistor to compensate for changes in the detection sensitivity of the Schottky diode with temperature.

20-MHz IF Assembly

The 20-MHz IF circuit (see Fig. 3) consists of a series of filters, amplifiers and attenuators that determine the bandwidth and power level of the 20-MHz noise signal sent to the noise power detector. Nominal bandwidth of the
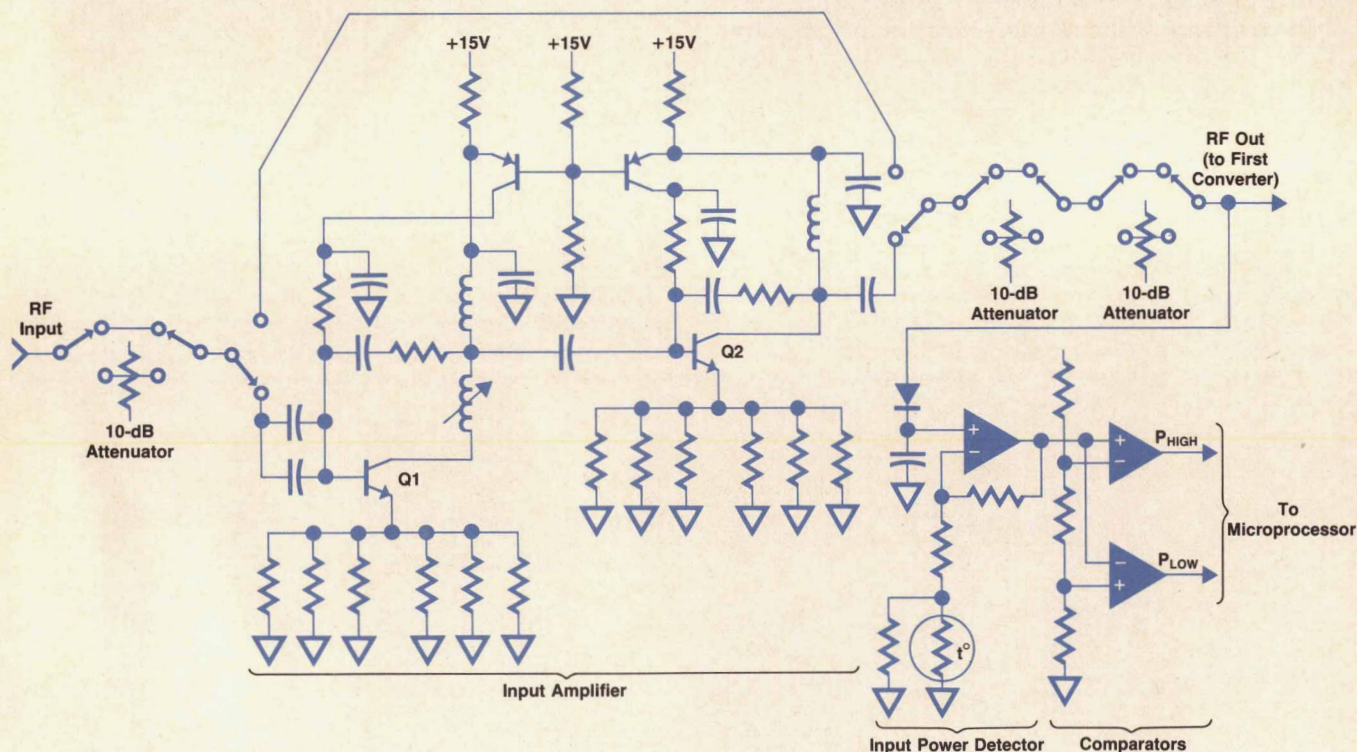

Fig. 4. The 8970A's input assembly serves as a low-noise, broadband, variable-gain front end. It consists of three 10-dB attenuators, a 20-dB amplifier, and a power detector.
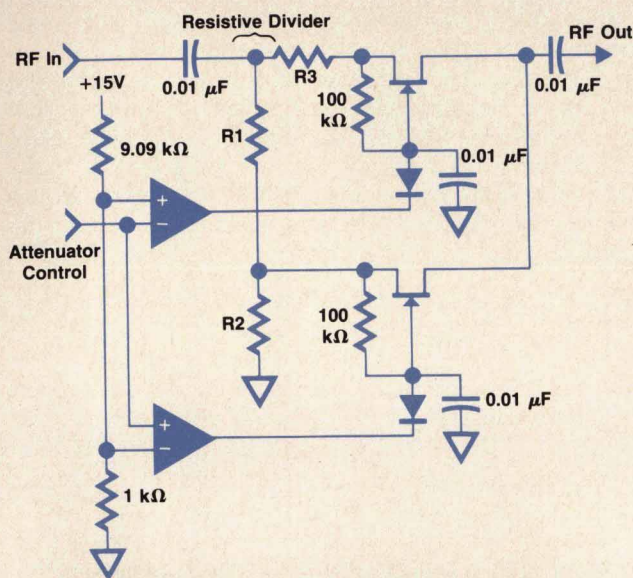
Fig. 5. An attenuator section representative of the 20, 10, and 5-dB step attenuators in the 20-MHz IF circuit.

complete circuit is about 4 MHz. Gain of the 20-MHz IF circuit is variable under control of the microprocessor in 5-dB steps from +40 dB to +75 dB. A detector is included in the IF circuit to detect feedthrough from the first LO when the LO is tuned near 2050 MHz during a frequency calibration.

The two bandpass filters at the front end of the 20-MHz IF circuit combine with the bandpass filter at the output of the 7-dB amplifier to form a composite eight-pole filter. These filters determine the nominal 4-MHz bandwidth of the
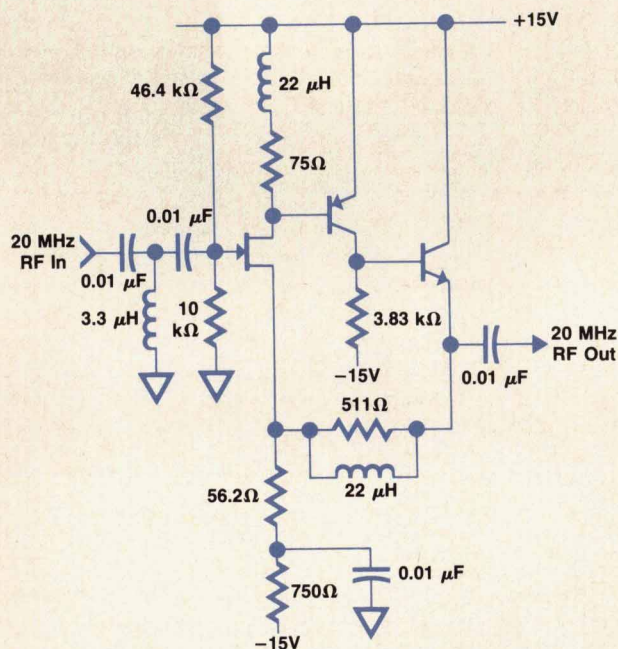
complete IF circuit. They also serve to reject unwanted first-LO feedthrough.

The 20, 10 and 5-dB attenuators are realized by simple resistive dividers that are switched by complementarily driven FET stages. A representative attenuator is shown in the schematic of Fig. 5. The state of the control line causes either the upper or the lower FET to be switched into the on state, thereby coupling either the unattenuated or the attenuated version of the input signal to the output. Resistor R3 causes the attenuator to present a nearly constant impedance to the following stage regardless of the attenuator's state. This nearly constant impedance minimizes the error resulting from loading by the following stage. This attenuation scheme was selected over a mechanically switched attenuator for reasons of cost, repeatability, and reliability.

The method chosen for attenuation imposes some requirements on the design of the amplifiers between the attenuator sections. Each of these amplifiers must have a low output impedance to appear as an ideal voltage-source driver for the resistive divider of the attenuator. Each amplifier must also have a high input impedance to minimize loading effects on the attenuator stage preceding it. The schematic for these amplifiers is shown in Fig. 6. The FET input transistor, feedback topology, and shunt resonating input inductor combine to realize the required high input impedance. The emitter follower output stage and feedback serve to lower the output impedance of the amplifier.

Frequency calibration of the 8970A is accomplished by tuning the first LO near 2050 MHz and then observing the resultant LO feedthrough by means of the frequency calibration detector located in the 20-MHz IF assembly (see Fig. 3). Feedthrough from the first LO is passed through a narrow bandpass filter centered in the 20-MHz IF passband. Output from this filter is detected, resulting in a dc level that is related to LO frequency. The maximum dc level corresponds to the center of the 20-MHz IF passband or zero instrument input frequency. If the LO is tuned below 2050 MHz and then stepped up in frequency, the output of the frequency calibration detector always increases in level relative to the preceding output until a maximum is reached at 2050 MHz. After this, the output begins to decrease. Only information about whether the output of the frequency calibration detector is increasing or decreasing is really necessary to locate the zero frequency point. This allows the use of an economical slope detector circuit (see Fig. 7). A
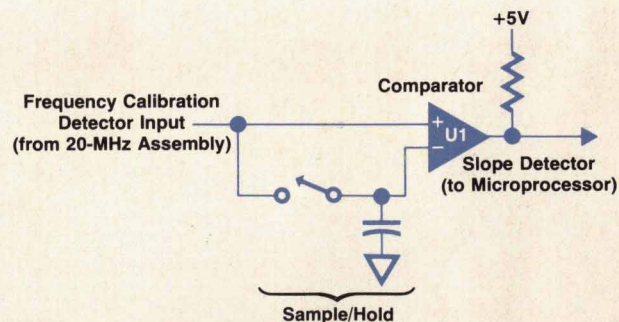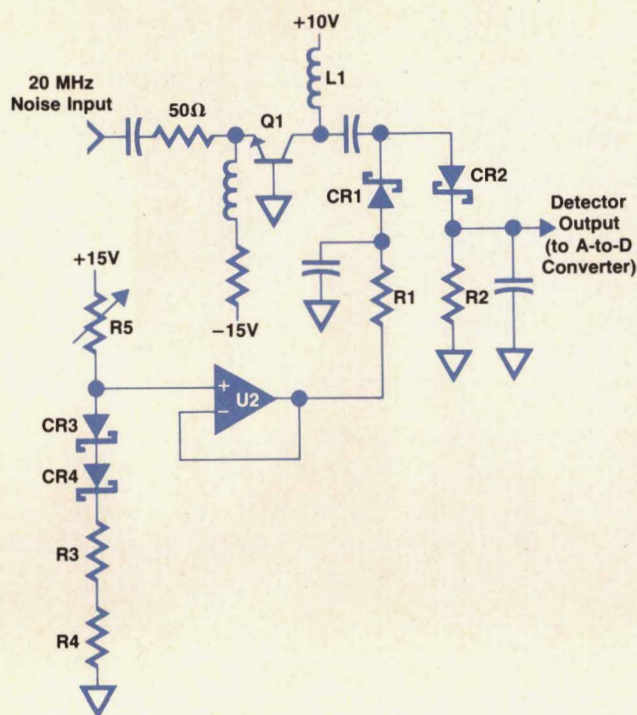

Fig. 6. Representative 20-MHz IF amplifier. Feedback creates a high input impedance and a low output impedance and determines the gain.

Fig. 7. A simple, economical slope detector is used in automatic frequency calibration.
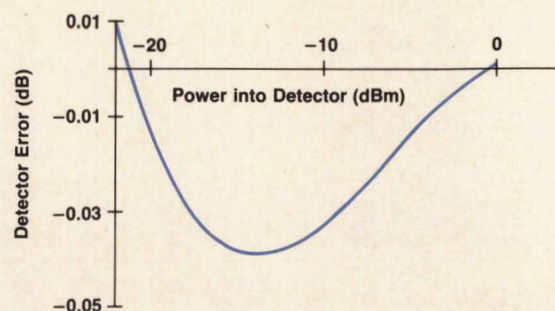
Fig. 8. *The noise power detector converts RF noise signals to dc levels that the microprocessor can measure by means of the analog-to-digital converter.*

Fig. 9. *Typical performance curve for the noise power detector.*

sample-and-hold circuit saves the previous output of the detector circuit and U1 compares it to the current output. As long as successive levels increase, U1's output to the controller remains in a high state. At the maximum detector output level the comparator switches state, signaling the controller that zero instrument frequency has been located.

Noise Power Detector Assembly

The noise power detector circuit, shown in Fig. 8, converts RF noise signals to dc levels that the controller can interpret by means of the analog-to-digital converter (ADC). The basic detector consists of a common-base transistor stage Q1 driving a pair of rectifying Schottky diodes CR1 and CR2. The common-base stage provides a good 50Ω termination for the last 20-MHz IF bandpass filter while at the same time functioning as a high-impedance current source driver for the detector diodes. Diode CR2 rectifies positive-going half-cycles, producing an average dc current in resistor R2. The resultant dc voltage across this resistor is the detected signal that is sent to the ADC and is proportional to the square root of the RF noise power. Diode CR1

and resistor R1 are present to provide a symmetrical load for the negative-going half-cycles. Inductor L1 resonates with the capacitance present at the collector of Q1 to realize more closely the high-impedance current source needed for the diodes.

Detector linearity is improved by biasing the diodes slightly. This is accomplished by applying a voltage to R1, CR1, CR2, and R2 with op amp U2. This voltage must be temperature compensated to ensure that detector sensitivity remains constant. R5 drives R3, R4, CR3, and CR4 with a constant current. The resultant voltage at the noninverting terminal of U2 is sensed by this unity-gain op amp stage and applied to the detector circuit.

The performance of the noise power detector is quite good. Its dynamic range extends from 0 dBm to about −22 dBm. Deviation from linearity over this range is less than 0.04 dB. A typical performance curve for the detector is shown in Fig. 9.

Applications

Fig. 10 shows an example of a VHF measurement using the 8970A Noise Figure Meter. The meter is making a swept measurement of gain and noise figure from 10 to 500 MHz. No additional amplifiers, local oscillators, filters, or mixers are needed. The 8970A is automatically correcting for ENR variations with frequency, using the correct T_C, and removing the second-stage noise. The results are digitally stored in memory and are refreshed at a rapid rate for display on a nonstorage oscilloscope.

To measure at frequencies above 1500 MHz, an external mixer and LO are required (Fig. 11). However, the 8970A controls the LO's frequency and level via the HP-IB. Thus all corrections can be made and the results digitally stored for the oscilloscope display. In this measurement the 8970A
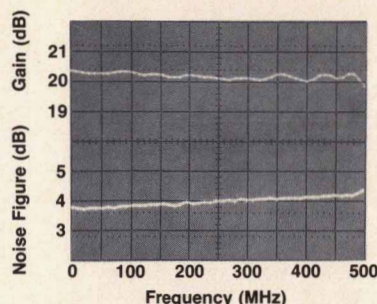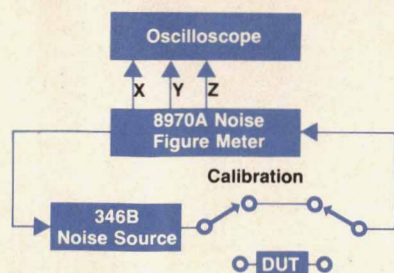
Fig. 10. *A swept measurement of gain and noise figure from 10 to 500 MHz.*
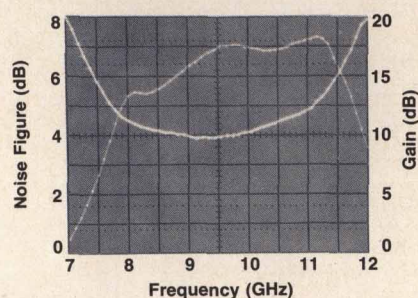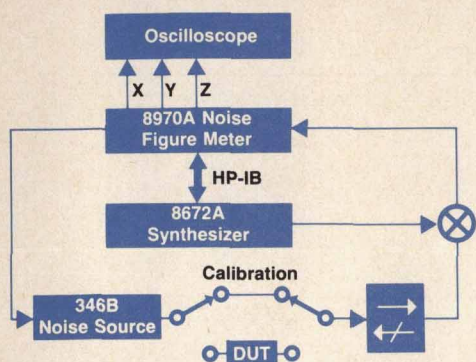
Fig. 11. *Using an external local oscillator (an HP 8672A) and mixer to measure above 1500 MHz.*

is tuned to 30 MHz and tunes the 8672A local oscillator from 7 to 12 GHz. An isolator in front of the RF port of the mixer reduces the mismatch uncertainty of the gain measurement and reduces the sensitivity of the mixer's noise figure to the output impedance of the device under test.

Electromagnetic interference (EMI) can cause errors of several dB. A spurious signal will add proportionally more power to the noise-source-off power measurement than to the noise-source-on measurement. This decreases the Y factor and thus increases the measured noise figure.

EMI can be detected by making swept noise figure measurements. For wide frequency sweeps, EMI appears as peaks at the frequencies of the spurious signals. Narrow sweeps over frequencies where a broad band of interference exists may show broad humps.

Fig. 12 shows the effect of EMI on a DUT that is not in a tightly shielded box. EMI can also enter through connectors (such as BNC), through single-shielded coax, or over the power supply leads, and can be picked up by tuners during transistor measurements.

Acknowledgments

Product manager Mike Cuevas' research paper helped launch the 8970A project. John Page, R&D manager during the project, encouraged us to go for a broad frequency range and external LO control via the HP-IB. Steve Adam was section manager during the development phase. Nick Kuhn, product marketing engineer, provided many valuable inputs that helped define the product. Mike Pozzi designed the digital and low-frequency circuits including the ADC and the CRT driver. Takashi Yoshida developed most of the 24K bytes of firmware. Tim Kelly and Patty Decker Morton did the product design. Production section manager Tom Neal assembled a fine crew including Sandi Molina, assembly supervisor, and Ray Lew, test supervisor, that achieved a smooth buildup to volume production. Production engineer Mark Haaland showed fine attention to detail in helping introduce the 8970A to production. Harry Bunting, production engineer, built the test system, provided advice on producibility, and helped in environmental testing.

References

1. H.C. Poulter, "An Automatic Noise Figure Meter for Improving Microwave Device Performance," Hewlett-Packard Journal, Vol. 9, no. 5, January 1958.
2. M.R. Negrete, "Additional Conveniences for Noise Figure Measurements," Hewlett-Packard Journal, Vol. 10, no. 6-7, February-March 1959.
3. R. Rosen, "LNA Sales Skyrocket as Prices Plummet," Microwaves, Vol. 21, no. 3, March 1982, pp. 17-22.
4. M.D. Roos, et al, "Add-on Digital Signal Processing Enhances the Performance of Network and Spectrum Analyzers," Hewlett-Packard Journal, Vol. 29, no. 5, January 1978.
5. M.G. Arthur, "The Measurement of Noise Performance Factors: A Metrology Guide," NBS Monograph No. 142.
6. R. Adler, et al, "Description of the Noise Performance of Amplifiers and Receiving Systems," Proceedings of the IEEE, Vol. 51, no. 3, March 1963, pp. 436-442.
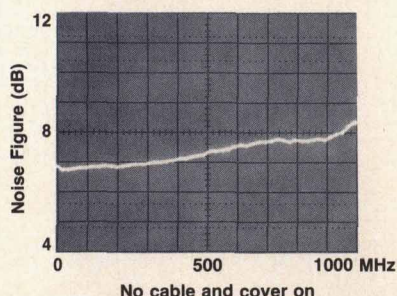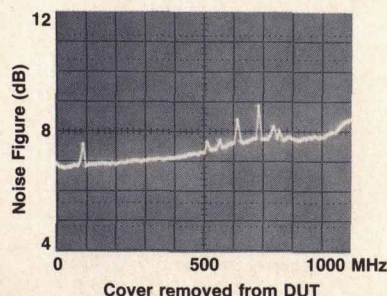
Fig. 12. *Electromagnetic interference appears as peaks during swept measurements of noise figure.*

Appendix
Noise Figure Basics

Noise limits the detection of weak signals. As a signal passes through each stage of a system, noise is added. Thus the signal-to-noise ratio is reduced. Noise figure is a measure of this degradation.

Two main mechanisms cause the noise that is responsible for the signal degradation measured by noise figure. The first is the random motion of charge carriers caused by thermal agitation. This noise is called thermal noise, Nyquist noise, or Johnson noise.[1,2] It exists in all conductors whose temperature is above absolute zero.

This thermal noise generates an available power of kTB where k is Boltzmann's constant, T is absolute temperature, and B is bandwidth. This is the power that can be delivered to a conjugately matched load. Note that the available thermal noise power is independent of the resistance R. If the resistor is at 290K, the available power is 4.00×10^{-21} watts (or -174 dBm) in a 1-Hz bandwidth.

The second mechanism is the random, corpuscular flow of carriers in transistors and diodes. Each charge carrier (electron or hole) is emitted individually and flows across the device on its own. Thus the current arriving at the collecting electrode is a series of little pulses randomly distributed in time, each having the charge of one electron. This is a noisy process, and the noise generated is called shot noise.[3]

Noise figure is defined as the total output noise of the device under test (DUT) caused by both the DUT and the source, divided by the output noise caused by the source alone.[4] Because this ratio depends on the amount of noise produced by the source, it is essential to specify that noise. Therefore, noise figure is defined referred to a source that has the available output noise power of a resistor at 290K.*

$$F = \frac{N_{out} \text{ caused by DUT} + N_{out} \text{ caused by source}}{N_{out} \text{ caused by source}} \Bigg|_{T_{source} = 290K}$$

Device noise can be modeled using the fact that the available noise power produced by a resistor is kTB. In Fig. 1a, the total output noise power is the sum of the noise caused by the source (kT_sB) and the noise added by the noisy amplifier with gain G. To model this added noise, the amplifier is made noiseless and an additional fictitious resistor is added at the input, as shown in Fig. 1b. The temperature of this resistor, T_e, is chosen so that the total output noise power remains the same as from the noisy amplifier in Fig. 1a. In this model, the power from both resistors is added, and neither loads the output of the other.

T_e is called the effective input noise temperature.[5] It is very useful in systems analysis and in specifying very low-noise components. The relationship between T_e and noise figure will be derived later.

To measure T_e, one might try connecting a power meter to the output of the device, measuring $P = k(T_s + T_e)BG$, and solving for T_e. However, BG is not usually known. B is really the noise bandwidth, which is the integral of the gain over frequency divided by the gain at the center of the band. In addition, it is difficult to measure absolute power accurately.

Because there are really two unknowns (T_e and BG), two independent equations are needed. Making another power measurement with the source resistor at a different temperature will yield a second equation, independent of the first. Thus P_2 and P_1 are measured with T_s equal to a hot (T_H) and a cold (T_C) temperature, respectively.

$$P_2 = k(T_H + T_e)BG$$

$$P_1 = k(T_C + T_e)BG$$

Dividing these two equations causes the unknown BG to cancel out. An added benefit is that only the ratio of two powers is required and not absolute power. This ratio is called the Y factor.

$$\frac{P_2}{P_1} = Y = \frac{T_H + T_e}{T_C + T_e}$$

Solving for T_e yields

$$T_e = \frac{T_H - YT_C}{Y - 1}$$

This involves only the two known source temperatures and the measured Y factor.

The definition of noise figure and the model of Fig. 1b are now used to express noise figure in terms of T_e. The model shows that the output noise caused by the device is kT_eBG, and the output noise caused by the source is kT_sBG. Because noise figure is referred to a source at 290K, the output noise caused by the source becomes k290BG.

Putting these into the definition and solving yields F in terms of T_e.

$$F = \frac{kT_eBG + k290BG}{k290BG}$$

*This definition applies only to single-input, single-output devices. For devices that have multiple inputs, outputs, and/or responses, see reference 4.

$$F = 1 + T_e/290$$

Inserting the equation for T_e gives F in terms of Y, T_H, and T_C.

$$F = 1 + \frac{T_H - YT_C}{290(Y - 1)}$$

$$F = \frac{(T_H/290 - 1) - Y(T_C/290 - 1)}{Y - 1}$$

10 log $(T_H/290 - 1)$ is defined as the excess noise ratio or ENR of the source. The T_H or on temperature of an electronic noise source is usually specified by its ENR.

$$ENR = 10 \log (T_H/290 - 1)$$

If the cold source temperature T_C is approximately 290K, then the second term in the numerator of the equation for F is approximately zero, and noise figure in dB simplifies to:

$$F_{dB} \approx ENR - 10 \log (Y - 1)$$

In general T_C is not 290K, and making this approximation can result in an error of 0.1 dB or more.

The method just described for measuring noise figure requires changing the effective temperature of the source from T_H to T_C. It is difficult and slow to heat a resistor physically. A solid-state noise source provides a convenient solution. The kT_HB noise is generated by avalanche breakdown in a diode driven by a constant current. The noise can be switched on and off by turning the current on and off. An attenuator at the output provides a good match and serves as the source of noise (kT_CB) when the diode is off.

Noise Figure of Cascaded Networks or Second-Stage Contribution

Noise contributed by stages following the device under test can cause an error in the measurement of noise figure. Again, this effect can be modeled using the concept of effective input noise temperature T_e. Because k and B will be the same everywhere, the noise powers can be simply modeled using temperatures only. Consider two cascaded amplifiers with gains G_1 and G_2 connected to a source at temperature T_s. Let T_{e1} and T_{e2} represent the noise added by the two amplifiers referred to their inputs, and let T_s represent the source noise. The total noise output of the cascaded system is $k(T_s + T_{e1})G_1G_2B + kT_{e2}G_2B$.

Next refer the noise of the second amplifier, T_{e2}, all the way back to the input of the first amplifier. To do this, divide T_{e2} by G_1, yielding T_{e2}/G_1.

Now the total effective input noise temperature, T_{eT}, is just the sum of all the noise temperatures except the source, T_s, at the input of the first amplifier.

$$T_{eT} = T_{e1} + T_{e2}/G_1$$

Solving $F = 1 + T_e/290$ for T_e and putting this in for each T_e yields the expression for the total noise figure for the cascaded network.

$$T_e = 290 (F - 1)$$

$$F_T - 1 = F_1 - 1 + (F_2 - 1)/G_1$$

$$F_T = F_1 + (F_2 - 1)/G_1$$

Thus, the second stage causes an error equal to $(F_2 - 1)/G_1$. This error can be removed if F_2 and G_1 can be measured. F_2 is easy to measure—just connect the noise source and read the result.
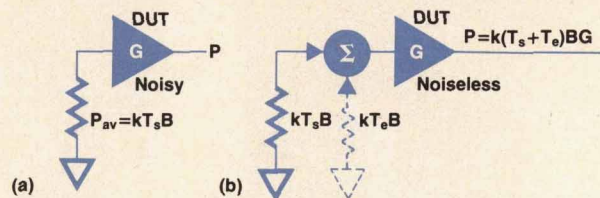
Fig. 1. *How effective noise temperature T_e is defined.*

How the 8970A Measures Gain

Gain measurement requires a little more work. All gain measurements require two steps: connect a signal source to a receiver and set a reference. Then insert the DUT and read the change in output power. The same thing can be done using a noise source as the signal source. However, because the "signal" power levels are so near the inherent noise levels, the noise figures of the DUT and meter must be taken into account. This yields four unknowns: T_{eD}, T_{eM}, G_D, G_M. Four power measurements are needed to set up four equations.

1. Connect noise source to 8970A
   Measure: $P_1 = k(T_C + T_{eM})BG_M$
   $P_2 = k(T_H + T_{eM})BG_M$

2. Insert DUT
   Measure: $P_3 = k(T_C + T_{eT})BG_DG_M$
   $P_4 = k(T_H + T_{eT})BG_DG_M$

T_{eM} and T_{eT} are eliminated by subtracting P_1 from P_2 and P_3 from P_4. Then kBG_M is eliminated by dividing the two differences. The result is the gain of the DUT, G_D, which can now be used in subtracting out the second-stage noise figure.

$$\frac{P_4 - P_3}{P_2 - P_1} = \frac{k(T_H - T_C)BG_DG_M}{k(T_H - T_C)BG_M}$$

$$G_D = \frac{P_4 - P_3}{P_2 - P_1}$$

This technique also allows the measurement of the noise figure and gain (loss) of devices whose gain is less than unity, such as mixers and attenuators.

References

1. J.B. Johnson, "Thermal Agitation of Electricity in Conductors," Physical Review, Vol. 32, July 1928, pp. 97-109.
2. H. Nyquist, "Thermal Agitation of Electric Charge in Conductors," Physical Review, Vol. 32, July 1928, pp. 110-113.
3. W. Schottky, "Spontaneous Current Fluctuations in Various Conductors," Annalen der Physik, Vol. 57, no. 23, 1918, pp. 541-567.
4. R. Adler, et al, "Description of the Noise Performance of Amplifiers and Receiving Systems," Proceedings of the IEEE, Vol. 51, no. 3, March 1963, pp. 436-442.
5. H.A. Haus, et al, "IRE Standards on Electron Tubes: Definition of Terms, 1962, (62 IRE 7.52)," Proceedings of the IEEE, Vol. 51, no. 3, March 1963, pp. 434-435.

Rick M. Cox
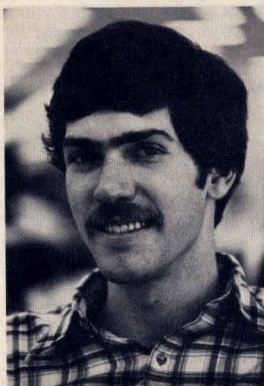
Rick Cox is electrical production engineering manager at HP's Spokane, Washington Division. Before moving to Spokane he was a design engineer with the Stanford Park Division, working on the design of the 8970A Noise Figure Meter. Born in San Juan, Puerto Rico, he grew up in St. Louis, Missouri and attended Washington University in St. Louis, receiving a pair of BS degrees in 1977, one in systems science and mathematics and the other in electrical engineering. In 1978 he received his MSEE degree from Stanford University. Rick is a baseball fan (the St. Louis Cardinals, of course), plays basketball and softball, and enjoys water and snow skiing, fishing, and boating. He lives in Spokane.

Howard L. Swain
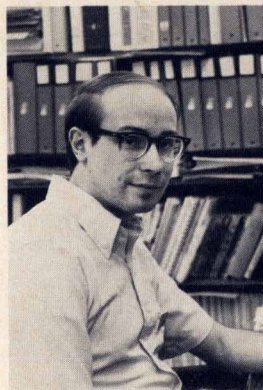
Howard Swain was project manager for the 8970A Noise Figure Meter. He received his BSEE degree from Iowa State University in 1969 and his MSEE from Stanford University in 1972. With HP since 1969, he has designed several low-noise oscillators and contributed to the design of the 8640B Signal Generator. He's a member of the IEEE and the author of a paper on accurate noise figure measurement techniques, and has been a guest lecturer at Stanford on RF amplifier design. Born in Des Moines, Iowa, he now lives in Palo Alto, California and enjoys square dancing, table tennis and playing a harpsichord and a pipe organ that he built from kits.

Laboratory Notebook

Mass Storage Unit Exerciser

TWO OEM PRODUCTS are used in the HP 4145A Semiconductor Parameter Analyzer.[1] One is the HP 1345A Graphic Display and the other is the flexible disc drive. To make it possible to service the entire instrument, methods must be provided for reliably isolating any faulty sections of these OEM products. The 1345A poses no problem for it has its own self-test capability. The flexible disc drive, however, does not. Therefore, the 4145A was designed to have a mass storage unit exerciser built-in for test and adjustment.

Interface Self-Test

To test the mass storage unit, the 4145A is put in the EXERCISER mode. Because the EXERCISER mode uses the mass storage unit interface circuit and its cables and connectors, these must be checked before the EXERCISER mode is enabled. This is done by the interface self-test, which also serves as a tool for isolating trouble between the interface and the disc drive. During the self-test, the service technician connects the interface connector for the disc drive to the test connector located on the edge of the motherboard (Fig. 1) to form loop-back signal paths. A special test ROM is then inserted in place of one of the normal 4145A system ROMs and the switches shown on the flexible disc controller board in Fig. 2 are
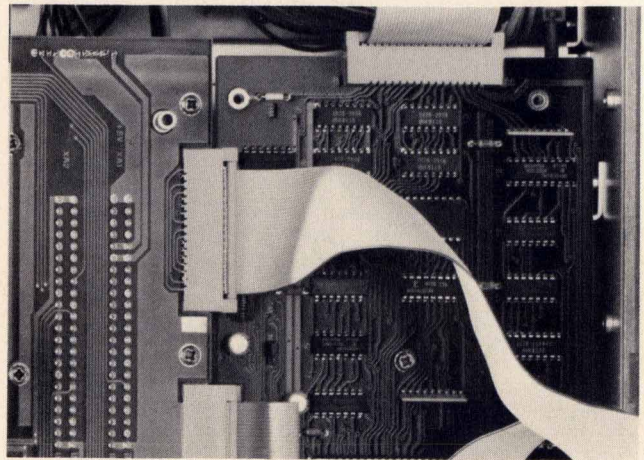
Fig. 1. *The mass storage unit interface in the 4145A can be tested by a service technician, who disconnects the cable to the disc drive and reconnects it to a loop-back board as shown in the upper left corner.*
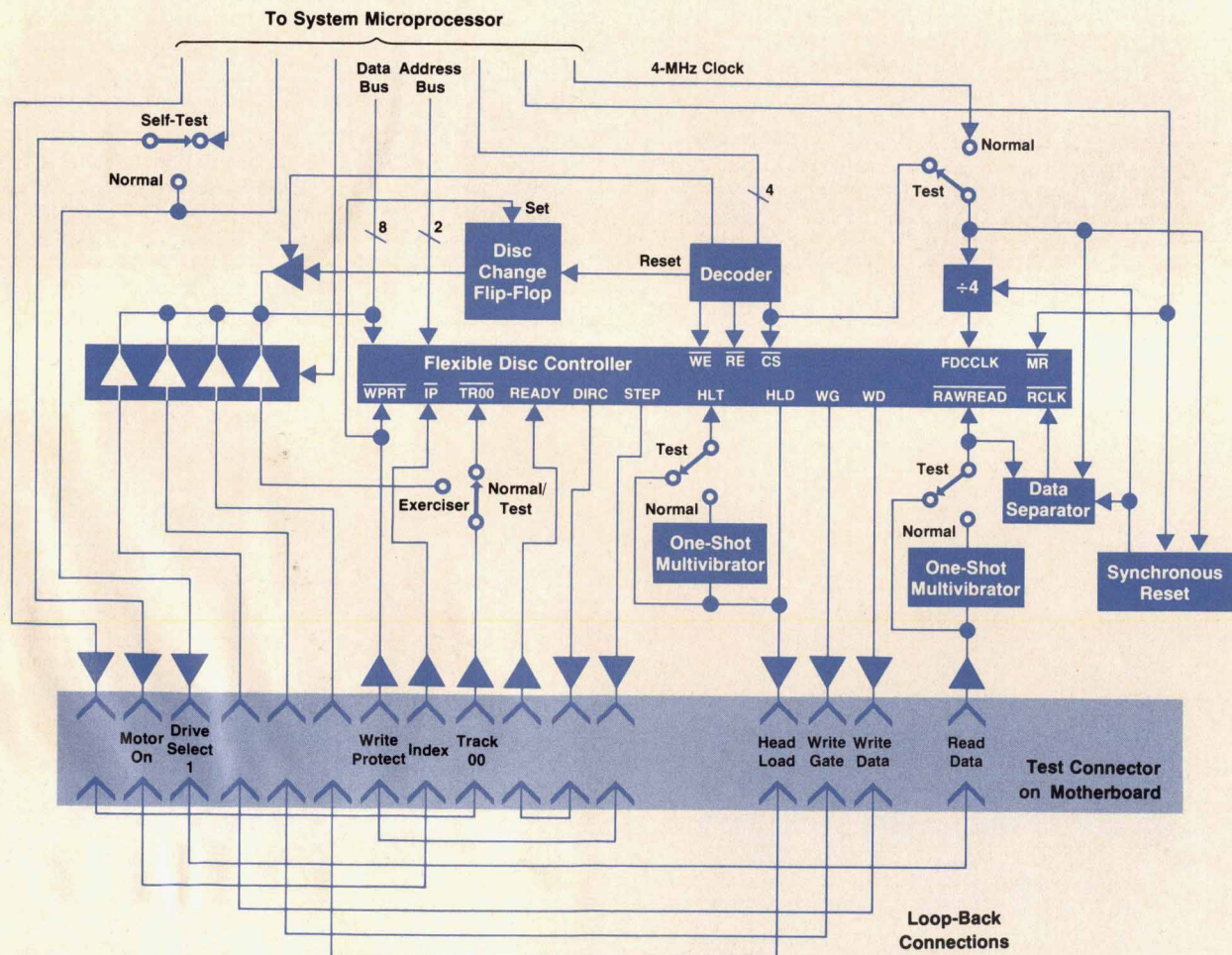
Fig. 2. *Self-test configuration for the mass storage unit interface.*

switched from NORMAL to TEST. The test ROM is supplied with the 4145A, mounted in an unconnected socket on one of the printed circuit boards.

Fig. 2 shows the test loop connection. This configuration was designed so that only a few additional components are used in the self-test mode to minimize any uncertainty introduced by them. The self-test checks the major functions of the flexible disc controller, including execution of step, read, and write commands, confirmation of the read/write data function using simulated data generated by the microprocessor, disc change, and the disc drive connectors and cables.

The test takes only seven seconds. In place of the 4-MHz clocks normally applied to the circuit, the chip select signal $\overline{CS}$ for the flexible disc controller is used in the test. By controlling the master reset $\overline{MR}$ of the flexible disc controller and using $\overline{CS}$ as a base clock, a completely synchronous check is performed. This also means that any trouble in the circuit can be isolated to the component level using digital signature analysis.

After the interface self-test, the technician reconnects the disc drive and enables the EXERCISER mode.

Exerciser

Fig. 3 shows the EXERCISER menu page, which is displayed on the CRT of the 4145A. TRACK NO. indicates the track number at which the read/write head is located when CAL is displayed along with the track number. If UNCAL is displayed, the read/write head has stepped out of track 00 or inside track 39, so the track number displayed is not guaranteed. WRITE PROTECT = ON(OFF) indicates whether the installed disc is write-protected or not. INDEX TIMING indicates disc rotational speed as determined by the time measured between INDEX pulses with the read/write head loaded. The seven softkey operations indicated along the right side of the menu are:

- TRACK 00. Moves the read/write head inward three steps and then outward until the track 00 switch turns on. The first three steps of step-in operation are required because, when the head is already out of the track 00 switch position, there is no chance of finding track 00 in step-out operation.
- STEP IN: Steps the read/write head toward track 39 (inward on the disc).
- STEP OUT: Steps the read/write head toward the lower-numbered tracks (outward on the disc). Track 00 switch status is read by the microprocessor through a buffer, but not through the flexible disc controller. This is because the controller terminates step-out operation when the track 00 signal is detected and does
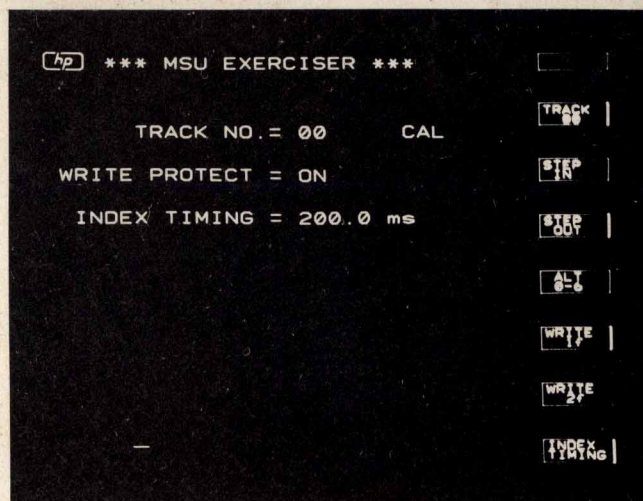
Fig. 3. The service technician tests the mass storage unit using an internal exerciser controlled through a special test ROM, the 4145A's CRT display, and softkeys. The display mode and softkey labels are shown above.

not allow the step-out operation over track 00 that is required in the drive check.
- ALT 0-6: Sets the drive to alternately move the read/write head between track 00 and track 06. This mode is used to check and adjust the track 00 switch.
- WRITE 1f: Hexadecimal data 00 is written on the specified track when this key is pressed.
- WRITE 2f: Hexadecimal data FF is written on the specified track when this key is pressed.
- INDEX TIMING: Displays the INDEX timing of the drive with 100-μs resolution. This is done by the system microprocessor, which checks the INDEX signal through the flexible disc controller while counting the 10-kHz clock.

The EXERCISER mode is one of the three modes of mass storage unit diagnostics stored in the test ROM. The other two modes are READ TEST and WRITE TEST, which are used to check for disc defects and to isolate trouble between the drive and the disc.

-Jin-ichi Ikemoto
Development Engineer

CHANGE OF ADDRESS: To change your address or delete your name from our mailing list please send us your old address label. Send changes to Hewlett-Packard Journal, 3000 Hanover Street, Palo Alto, California 94304 U.S.A. Allow 60 days.

5953-8510